RSC Advances

ROYAL SOCIETY OF CHEMISTRY

www.rsc.org/advances

Synthesis, Characterization and Computational Study of Potential Itaconimide-based Initiators for Atom Transfer Radical Polymerization

Chetana Deoghare[1], C. Baby[2], Vishnu S. Nadkarni[3], Raghu Nath Behera[1,*] and Rashmi Chauhan[1,*]

[1]Department of Chemistry, Birla Institute of Technology and Science, Pilani – K. K. Birla Goa Campus, Zuarinagar - 403726, Goa, India

[2]Sophisticated Analytical Instrument Facility, Indian Institute of Technology Madras, Chennai, Tamilnadu - 600036, India

[3]Department of Chemistry, Goa University, Taleigao Plateau, Goa - 403206, India

*Corresponding – (RNB) rbehera@goa.bits-pilani.ac.in, Tel: +91 832 2580331, Fax: +91 832 2557033; (RC) rchauhan@goa.bits-pilani.ac.in, Tel: +91 832 2580153, Fax: +91 832 2557033

Abstract: The atom transfer radical polymerization (ATRP) has been a promising technique to provide polymers with well defined composition, architecture and functionality. In most of the ATRP processes, alkyl halides are used as an initiator. We report the synthesis of three possible potential initiators, *N*-phenyl(3-bromo-3-methyl)succinimide, *N*-phenyl(3-bromo-4-methyl)succinimide and *N*-phenyl(3-bromomethyl)succinimide for ATRP of *N*-phenylitaconimide (PI) and methyl methacrylate (MMA). These functionalized alkyl halides, having structural similarity with PI are characterized by FT-IR, HRMS, ^{1}H, ^{13}C NMR spectroscopy and elemental analysis. The equilibrium constants for the ATRP activation/ deactivation process (K_{ATRP}) of these alkyl halides along with a commercial ATRP initiator (ethyl-α-bromoisobutyrate) are determined using UV-Vis-NIR and DOSY NMR spectroscopy. Alternatively, these compounds along with some similar alkyl halides (R–X) are investigated using density functional theory for their possible chain initiation activity for the ATRP process. The B3LYP functional and 6-31+G(d)/ LanL2DZ basis set is used for the prediction of geometries and energetics associated with the homolytic R–X bond dissociation. The relative value of K_{ATRP} and its variation with system parameters (such as, substituent, temperature and solvent) is investigated. We find a good agreement between the experimentally determined and theoretically calculated K_{ATRP} values. Our experiments show that the newly synthesized initiator

N-phenyl(3-bromo-3-methyl)succinimide performs better than the commercially available initiator ethyl-α-bromoisobutyrate for the atom transfer radical copolymerization of PI and MMA.

Keywords: ATRP, *N*-phenylitaconimide, Density functional theory, Homolysis.

INTRODUCTION

Atom transfer radical polymerization (ATRP)[1] is one of the popular and robust controlled radical polymerization (CRP) technique for the preparation of polymers with controlled architecture and site specific functionality. Like other CRP methods,[2-5] ATRP is controlled by equilibrium between propagating radicals and dormant species (mostly in the form of initiating alkyl halides or macromolecular species).[6] Various types of initiators have been used in ATRP,[2, 7-8] e.g. halogenated alkanes, benzylic halides, α-haloesters, α-haloketones, α-halonitriles, sulfonyl halides, and iniferters. The basic mechanism of ATRP process (**Scheme 1**) involves homolytic cleavage of alkyl halide (R–X) bond (activation step) by a transition metal complex in its lower oxidation state (the activator, M_t^nY/L) generating (with rate constant of activation, k_{act}) reversibly the propagating radical ($R^\bullet$) and the transition metal halide complex in its higher oxidation state (the deactivator, $X–M_t^{n+1}Y/L$). In the deactivation step (with rate constant of deactivation, k_{deact}), the halide atom (X) is transferred back from the activator to the propagating radical, also through homolytic bond dissociation.[9]

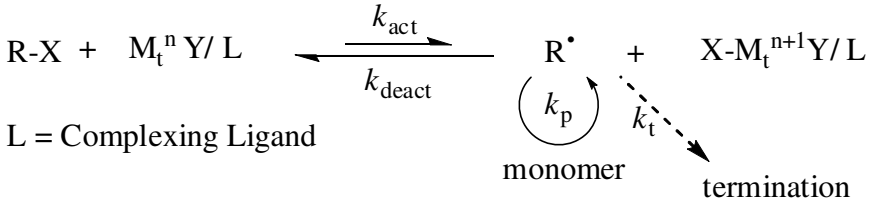

Scheme 1. Mechanism of Transition-Metal-Catalyzed ATRP.

A successful ATRP process needs to have a uniform growth of all the chains and small contribution of terminated chain. This can be achieved through fast initiation and rapid reversible deactivation and also by preserving the chain end functionality.[10] An efficient ATRP initiator should have the rate of initiation faster than the rate of propagation, and have minimum side

reactions. On the other hand, very reactive initiator may provide too many radicals which will terminate in early stage and slowdown the overall process. Thus, the initiator reactivity should be comparable to the monomer reactivity. One way of achieving this is to employ initiator that structurally mimics the dormant species.[2, 6, 11] To obtain a well defined polymer with narrow molecular distribution, the halide group must rapidly and selectively migrate between the growing chain and the transition metal complex (the catalyst). Thus, the initiator should be carefully selected in accordance with the structure and reactivity of the monomers and metal complexes.[12] A normal ATRP process has one notable limitation that the catalysts used are sensitive to air and other oxidant.[13] In order to overcome this drawback, Matyjaszewski's group[14] has developed an improved ATRP technique, namely activator generated by electron transfer atom transfer radical polymerization (AGET - ATRP). In a typical AGET - ATRP system, a transition metal complex in its higher oxidation state such as Cu^{II} complex is used as catalyst instead of Cu^{I} complex for normal ATRP system. The Cu^{I} complex is generated *in situ* from Cu^{II} complex using reducing agent such as tin(II)-ethylhexanoate.[14a]

Several experimental[15] as well as theoretical[15b,16] studies have reported the kinetic and thermodynamic parameters of ATRP for various systems. The rate of an ATRP process depends on the concentration of monomer [M] and propagating radical [$P^{\bullet}$]. The radical concentration depends on the position of the equilibrium and equilibrium constant of ATRP ($K_{ATRP} = k_{act} / k_{deact}$). Experimentally, K_{ATRP} can be determined from the polymerization kinetics. For example, in a $Cu^{I}Y$/ L (Y = Cl/ Br) catalyzed polymerization reaction when excess of the deactivating species (X-Cu^{II}L) is used and the concentration of other species such as activator, initiator and monomer do not change significantly, the rate of propagation (R_p) is given as,[17]

$$R_p = k_p[M]\,[P^{\bullet}] = k_p K_{ATRP}[M][I]_0 \times [Cu^{I}Y/\,L]/\,[X\text{-}Cu^{II}L] \quad \ldots\ldots\ldots\ldots\ldots\ldots (1)$$

Where k_p = rate constant of propagation, $[I]_0$ = initial concentration of initiator R-X and [Cu^{I}] = concentration of activator. Using this equation (Eq. 1) K_{ATRP} can be determined provided k_p is known.

Alternatively, K_{ATRP} can also be determined from the rate of formation of a dormant species/ persistent radical using Fischer - Fukuda equation for the persistent radical effect (Eqs. 2 and 3),[15b, 18]

$$Y = (6k_t K_{ATRP}^2 I_0^2 C_0^2)^{1/3} t^{1/3} \text{.....(2)}$$

$$R = \left(\frac{K_{ATRP} I_0 C_0}{6k_t}\right)^{1/3} t^{-1/3} \text{ .....(3)}$$

Or, its modification,[15b, 19] that take into account the changes in catalyst and initiator concentration (Eqs. 4-6)

$$F(Y) = 2k_t (K_{ATRP})^2 t + c' \text{ .....(4)}$$

Where, $F(Y) = \left(\frac{I_0 C_0}{C_0 - I_0}\right)^2 \left(\frac{1}{C_0^2 (C_0 - Y)} + \frac{2}{I_0 C_0 (C_0 - I_0)} ln\left(\frac{I_0 - Y}{C_0 - Y}\right) + \frac{1}{I_0^2 (C_0 - Y)}\right)$ for $C_0 \neq I_0$.....(5)

And, $F(Y) = \frac{C_0^2}{3(c_0 - Y)^3} - \frac{C_0}{(C_0 - Y)^2} + \frac{1}{C_0 - Y}$ for $C_0 = I_0$.....(6)

In the above equations, Y = concentration of deactivating species (X-Cu^{II}L), I_0 = initial concentration of initiator (R-X), C_o = initial concentration of catalyst (Cu^{I}Y/ L), R is the concentration of radical ($R^{\cdot}$), k_t is the termination rate constant, and t is time. The K_{ATRP} can be calculated (Eq. 4), from the slope of the plot $F(Y)$ vs t $\left(K_{ATRP} = \sqrt{\frac{slope}{2k_t}}\right)$, provided k_t is known.

Theoretically, the relative values of K_{ATRP} can be estimated from the homolytic bond dissociation energy (BDE) of the initiating R–X under certain conditions.[20] The atom transfer equilibrium of ATRP process,

$$\text{R-X} + \text{M}_t^n\text{Y/ L} \underset{}{\overset{K_{ATRP}}{\rightleftharpoons}} \text{R}^{\cdot} + \text{X-M}_t^{n+1}\text{Y/ L} \text{ .....(7)}$$

can be viewed as the sum of the following two equilibrium processes,[7, 9] viz. (i) homolytic bond dissociation of alkyl halide (Eq. 8) and (ii) X–M_t^{n+1}Y/ L bond formation (*halidophilicity*, Eq. 9), so that $K_{ATRP} = K_{RX} \times K_X$.

$$\text{(i)} \quad \text{R-X} \underset{}{\overset{K_{RX}}{\rightleftharpoons}} \text{R}^{\cdot} + \text{X}^{\cdot} \text{ .....(8)}$$

$$\text{(ii)} \quad \text{M}_t^n\text{Y/ L} + \text{X}^{\cdot} \underset{}{\overset{K_X}{\rightleftharpoons}} \text{X-M}_t^{n+1}\text{Y/ L} \text{.....(9)}$$

The value of the equilibrium constant K_X depends on the type of catalyst/ ligand (M_t^nY/ L) and halogen, X. For similar conditions and using the same catalytic system (similar K_X), the overall equilibrium constant K_{ATRP} will depend on the energetics of alkyl halide R-X, and a knowledge of the equilibrium constant K_{RX} alone will enable to predict the relative value of K_{ATRP}.[9, 20a, 20b]

Several studies have been done on ATRP of methyl methacrylate (MMA) using ethyl-α-bromoisobutyrate (**4**-Br) as initiator.[21] We are interested in the copolymerization of *N*-phenylitaconimide (PI) and MMA. Recently, we use ATRP method to copolymerize PI with MMA (in anisole at 80 °C using CuBr/ bipyridine catalyst) using the commercially available initiator **4**-Br, which resembles one of the monomers, MMA.[22] The molecular weight of the obtained copolymer was found to be less (3412 g/ mol) than that obtained by conventional polymerization method (23,300 g/ mol).[23] One of the reasons could be the chosen initiator. Previous studies[23, 24] on such kind of copolymer systems have shown higher reactivity ratios for itaconimides monomers as compared to MMA. This necessitates the need to explore de novo initiators for ATRP of PI and MMA. It will be of interest to copolymerize the same system with different initiators obtained from renewable resources having structural similarities with the other monomer (i.e. the itaconimide).

In this paper, we report the synthesis of three alkyl halides [*N*-phenyl(3-bromo-3-methyl)succinimide, *N*-phenyl(3-bromo-4-methyl)succinimide and *N*-phenyl(3-bromomethyl)succinimide] having structural similarity to PI. These alkyl halides are prepared from itaconic acid.[25] The K_{ATRP} values of synthesized alkyl halides and **4**-Br are determined using UV-Vis-NIR spectroscopy. These alkyl halides (along with some similar halides and some well known ATRP initiators) are also investigated using density functional theory (DFT) before attempting them as initiators for the ATRP copolymerization. The predicted initiator *N*-phenyl(3-bromo-3-methyl)succinimide has been successfully tested for the copolymerization of PI and MMA via AGET - ATRP process.

EXPERIMENTAL SECTION

Chemicals and Materials

Itaconic acid (99.0%) and phosphorus pentoxide (95.0%) were used as supplied, chloroform (99.5%), acetic anhydride (98%), aniline (99.5%) and acetone (99.0%) were purified by

distillation. Anhydrous sodium acetate (99.5%) was dried over flame. Silica gel for column chromatography was used as supplied. Dichloromethane (DCM, 99.0%) and toluene (99.0%) were dried using fused calcium chloride and was purified by distillation. 2,2'-bipyridine (Bpy) (99.5%), and acetonitrile dry (99.5%) was used as supplied. All the above chemicals were obtained from S. D. Fine Chem Limited, Mumbai, India. Itaconic anhydride (**I**) was synthesized from itaconic acid using the known methods reported in literature.[26] HBr gas was prepared by the bromination of 1,2,3,4-tetrahydro-naphthalene (99.0%, Sigma-Aldrich, Bangalore, India) and bromine (95.0%, S. D. Fine Chem Limited, Mumbai, India) using literature known procedure.[27] Ethyl-α-bromoisobutyrate (98.0%), $CuBr_2$ (99.9%, and tin(II) ethylhexanoate [$Sn(EH)_2$] (95.0%) were obtained from Sigma-Aldrich Chemicals Private Limited, Bangalore, India and used as supplied. CuBr (99.9%, Sigma-Aldrich Chemicals Private Limited, Bangalore, India) was purified by stirring overnight in glacial acetic acid and washing with absolute ethanol and diethyl ether, followed by drying under vacuum. Methyl methacrylate (99.0%, S. D. Fine Chem Limited, Mumbai, India) was purified by washing with 5%NaOH solution to remove the inhibitor followed by repeated washing with distilled water until it became neutral. It was then kept on anhydrous magnesium sulfate to remove the traces of water followed by vacuum distillation with calcium hydride. Anisole (99.0%, SRL Private limited, Mumbai, India) was purified by washing with 5% NaOH solution and then by distilled water. It was then kept on anhydrous potassium carbonate to remove the traces of water followed by vacuum distillation over sodium benzophenone.

The FT-IR spectra were recorded on a Shimadzu DR-8031 FT-IR spectrophotometer in the region 4000 to 400 cm^{-1} using KBr pellet. The ^{1}H NMR and ^{13}C NMR spectra were obtained by dissolving the samples in deuterated chloroform ($CDCl_3$) using a Brucker AV III 500 MHz FT-NMR and a Brucker DRX500 spectrometer, respectively. Chemical shifts (δ) are given relative to tetramethylsilane (TMS). Diffusion Ordered Spectroscopy (DOSY) NMR measurements were performed on a Bruker Avance (AV III) 500 MHz NMR spectrometer, equipped with a 5-mm broadband observe (BBO) z-axis gradient probe which delivers a maximum gradient strength of 50 G/cm. Experiments were carried out with active temperature regulation, at 25 ºC. Self diffusion coefficients were measured using the stimulated echo, bipolar gradient (stebpgp1s) pulse sequence. Generally, the diffusion coefficient (D) is experimentally determined by

monitoring the signal intensity decay in a 1D pulsed-field gradient spin-echo experiment (PFGSE) spectrum as a function of the applied gradient strength.[28] In the two dimensional DOSY experiment,[29, 30] the decay of magnetization as a function of increasing gradient intensity (i.e., the gradient ramp) is observed. The gradient ramp in our experiment was adjusted between 2 and 95% strength of the gradient amplifier using 16 equidistant steps. Each experiment was acquired with a spectral width of 4500 Hz and 16k complex points. The diffusion time (Δ) of 100 ms is used and the duration of the gradient pulse (δ) was 1ms. After Fourier Transformation and baseline correction, the spectra were processed with DOSY processing tools from Bruker Topspin 2.1 package. Data were analyzed using the variable gradient fitting routines, and in all cases the proton resonances were fit with a single exponential decay function using peak intensities. HRMS was recorded using 1290 Infinity UHPLC System, 1260 infinity Nano HPLC with Chipcube, 6550 iFunnel Q-TOF. Elemental analysis of the compounds was done using Vario Micro Cube elemental analyzer. The spectroscopic measurements were performed on Jasco V-570, UV-Vis-NIR spectrometer. Molecular-mass characteristics of the copolymers were determined by gel permeation chromatography (GPC) in THF as an eluent at flow rate of 0.75 mL/ min and column temperature of 25 ºC with a Agilent 1260 HPLC-GPC system equipped with column: PL gel 5 micron Mixed D: 300 mm × 7.5 mm with a differential refractometer. Polystyrene standards with molecular weight of 10^3 to 10^5 g/ mol are used for calibration.

Computational Details

Gaussian09[31] was used as source program for all theoretical calculations. All the geometries were fully optimized using the hybrid B3LYP exchange correlation functional[32] with 6-31+G(d) basis set, except for Iodine, where we use LanL2DZ basis set. Frequency calculations were performed for all the compounds to check (no imaginary frequencies) the stationary points as minima on the potential energy surface. The scaling factor used for frequency calculation was 0.9613.[33] We have used Gauge-Independent Atomic Orbital (GIAO) method inbuilt in Gaussian09 software for computing NMR properties. All the ^{1}H NMR calculations were carried out with HF/6-311+G(2d,p) method from B3LYP/6-31+G(d) optimized geometry. All the systems containing unpaired electron were optimized with spin unrestricted formalism. The spin contamination was found to be negligible (the mean value of the S^2 operator was close to the theoretical value of 0.75 for all radicals). A spin-orbit correction term was applied for X = Cl, Br

and I due to their atomic nature.[34] The DFT calculation includes only the average energy of the ground state ^2P term, the extra stability of the real ground-state $^2P_{3/2}$ term is taken from the literature values (0.8, 3.5 and 7.3 kcal/mol for Cl, Br and I respectively).[35] Solvent effects were studied using Tomasi's polarizable continuum model (PCM).[35]

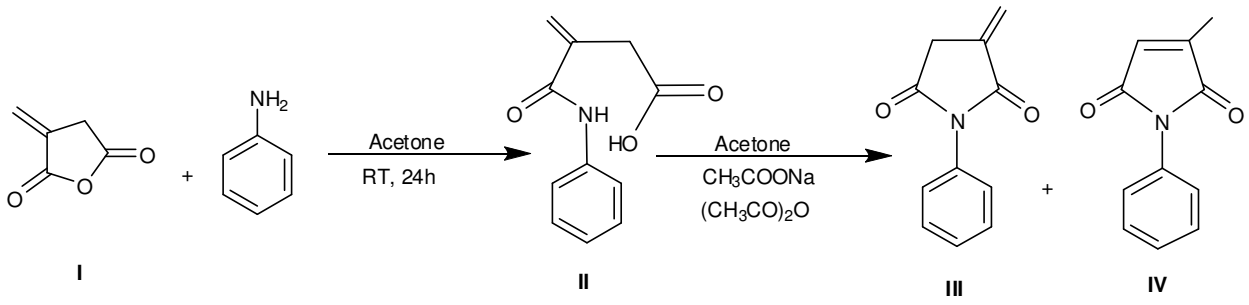

Scheme 2. Synthesis of *N*-phenylitaconimide (III) and *N*-phenylcitraconimide (IV).

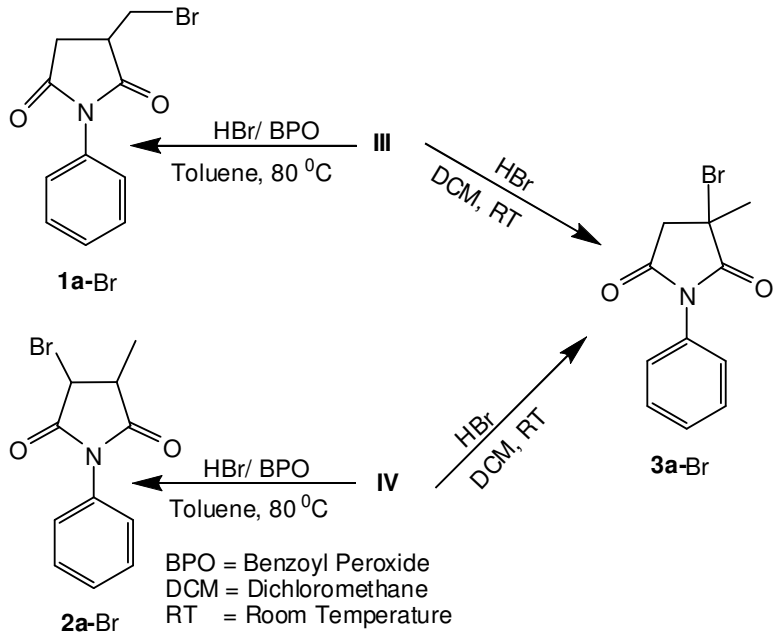

Scheme 3. Synthesis of Bromo Substituted Succinimides.

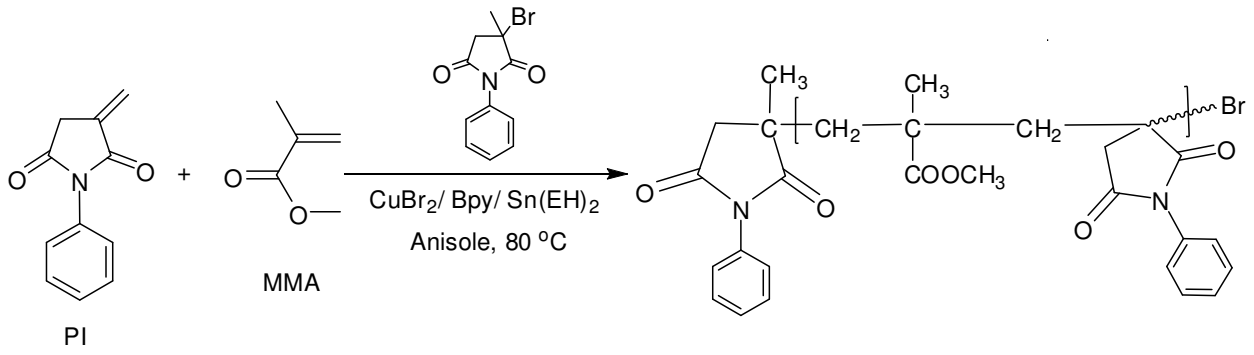

Scheme 4. Reaction Scheme for the Synthesis of Copolymer of PI and MMA via AGET - ATRP Using 3a-Br **as Initiator.**

A. Synthesis of Compounds II – IV (Scheme 2)

1. Synthesis of *N*-phenylitaconamic acid (**II**):

In one litre of kettle equipped with a mechanical stirrer, **I** (30 g, 0.27 mol) dissolved in 100 mL of acetone was taken. To this solution Aniline (25 mL, 0.27 mol), dissolved in 100 mL of acetone was added slowly with vigorous stirring. The *N*-phenylitaconamic acid starts precipitating out. The stirring was continued for another 12h. The obtained precipitate was filtered, dissolved in saturated solution of sodium bicarbonate and reprecipitated with 5 M HCl. The precipitate was filtered, washed with distilled water and dried in oven at 80 °C giving **II**, (19.0 g, Yield 63%, mp 145-150 °C).

2. Synthesis of *N*-phenylitaconimide (**III**) and *N*-phenylcitraconimide (**IV**):

To the solution of **II** (25 g, 0.14 mol) in 100 mL of acetone, acetic anhydride (25 mL, 0.25 mol) and anhydrous sodium acetate (10 g, 0.12 mol) were added. The reaction mixture was refluxed until a clear solution was obtained. Refluxing with stirring was continued for another 5h. The reaction mixture was then cooled to room temperature and poured in excess of ice cold water. The precipitate obtained was filtered and washed with saturated solution of sodium bicarbonate followed by distilled water. The crude product was purified by column chromatography using 10% ethyl acetate in hexane as the eluent giving **III** and **IV**.

N-phenylitaconimide (**III**), (12.5g, Yield 50%, mp 115 °C):

IR (KBr, cm^{-1}): 3098 (aromatic C-H stretch), 3050 (alkenyl C-H stretch), 2994, 2955 (C-H stretch), 1789 and 1714 (>C=O of imide), 1663 (>C=C< stretch of double bond in ring), 1593, 1501, 1453 (aromatic >C=C< stretch), 761 (oop C-H bending).

^{1}H NMR ($CDCl_3$) δ: 7.4 (m, 2 H, C_6H_5), 7.3 (m, 2 H, C_6H_5), 7.2 (m, 1 H, C_6H_5), 6.4 (m, 1 H, H1 of vinylic CH_2), 5.6 (m, 1 H, H2 of vinylic CH_2), 3.4 (m, 2 H, CH_2 of ring).

N-phenylcitraconimide (**IV**), (6.2 g, Yield 25%, mp 100 °C):

IR (KBr, cm^{-1}): 3082 (aromatic C-H stretch), 3069 (alkenyl C-H stretch), 2923 (C-H stretch), 1701 and 1717 (>C=O of imide), 1641 (>C=C< stretch of double bond in ring), 1593, 1505, 1409 (aromatic >C=C< stretch), 876 (oop C-H bending).

^{1}H NMR ($CDCl_3$) δ: 7.4 (m, 2 H, C_6H_5), 7.3 (m, 2 H, C_6H_5), 7.2 (m, 1 H, C_6H_5), 6.4 (q, 1 H, ^{3}J = 1.6 Hz, CH), 2.1 (d, 3 H, ^{3}J = 1.6 Hz, CH_3).

The FT-IR and ^{1}H NMR spectra of compounds **III** and **IV** are given in Supporting Information Figure S1 to Figure S4. The detailed characterization of compounds **III** and **IV** is reported in literature.[23, 36]

B. Synthesis of Bromo Substituted Succinimides (Scheme 3)

3. Preparation of *N*-phenyl(3-bromomethyl)succinimde (**1a**-Br):

To the solution of **III** (2 g, 0.01 mol) in 50 mL of toluene, HBr gas was purged for 24h at 80 ºC temperature in presence of benzoyl peroxide. The stirring was continued for 12h. The crude product obtained by concentrating the reaction mixture using rotary evaporator was purified by column chromatography using petroleum ether and diethyl ether as solvent system followed by crystallization from DCM and hexane. The compound was dissolved in minimum amount of DCM and hexane was added drop wise till the solution was turbid. The mixture was then kept in ice to get **1a**-Br (1.0 g, Yield 50%, mp 177 °C).

IR (KBr, cm^{-1}): 3069 (aromatic C-H stretch), 1784, and 1703 (>C=O of imide), 1590, 1491, and 1447 (aromatic >C=C< stretch), 758 (oop C-H bending), 595 (C-Br stretch).

^{1}H NMR ($CDCl_3$) δ: 7.3 (m, 1 H, C_6H_5), 7.4 (m, 2 H, C_6H_5), 7.5 (m, 2H, C_6H_5), 4.0 (dd, 1 H, ^{1}J = 8.4 Hz, ^{2}J = 4.5 Hz, CH_2), 3.7 (dd, 1 H, ^{1}J = 8.4 Hz, ^{2}J = 3.5 Hz, CH_2), 3.5 (m, 1 H, CH), 2.9 (dd, 1 H, ^{1}J = 14.8 Hz, ^{2}J = 5.0 Hz, CH_2), 3.1 (dd, 1 H, ^{1}J = 14.8 Hz, ^{2}J = 9.5 Hz,CH_2).

^{13}C NMR (125 MHz, $CDCl_3$) δ: 175.81 and 174.52 (>C=O), 129.33, 128.97, 128.52, and 131.74 (C_6H_5), 41.20 (CH_2Br), 33.38 (CH), 32.32 (CH_2).

Elemental analysis (CHNOBr): Found - %C, 49.02; %H, 3.71; %N, 5.13; %O, 11.88; %Br, 30.26; Calculated for $C_{11}H_{10}NO_2Br$: %C, 49.28; %H, 3.76; %N, 5.22; %O, 11.94; %Br, 29.80.

HRMS (EI): (*m/z*) 267.7751 ($[M]^+$; 95%), 269.4687 ($[M+2]^+$; 90%); Calculated mass for $C_{11}H_{10}NO_2Br$; 268.1066, Observed mass for $C_{11}H_{10}NO_2Br$; 268.6219.

4. Preparation of *N*-phenyl(3-bromo-4-methyl)succinimide (**2a**-Br):

To the solution of **IV** (2 g, 0.01 mol) in 50 mL of toluene, HBr gas was purged for 24h at 80 ºC temperature in presence of benzoyl peroxide. The stirring was continued for 12h. The crude product obtained by concentrating the reaction mixture using rotary evaporator was purified by column chromatography using petroleum ether and diethyl ether as solvent system followed by crystallization from DCM and hexane. The compound was dissolved in minimum amount of DCM and hexane was added drop wise till the solution was turbid. The mixture was then kept in ice to get **2a**-Br (1.3 g, Yield 65%, mp 116 °C).

IR (KBr, cm^{-1}): 3077 (aromatic C-H stretch), 1791 and 1716 (>C=O of imide), 1591, 1501 and 1444 (aromatic >C=C< stretch), 763 (oop C-H bending), 520 (C-Br stretch).

^{1}H NMR ($CDCl_3$) δ: 7.3 (m, 1 H, C_6H_5), 7.4 (m, 2 H, C_6H_5), 7.5 (m, 2H, C_6H_5), 4.9 (d, 1 H, ^2J = 7.6 Hz, CH), 3.3 (m, 1 H, CH), 1.5 (d, 3 H, ^2J = 7.2 Hz, CH_3).

^{13}C NMR (125 MHz, $CDCl_3$) δ: 174.74 and 171.65, 131.45, 129.37, 129.07 and 126.28 (C_6H_5), 48.29 (C-Br), 40.68 (CH), 14.47 (CH_3).

Elemental analysis (CHNOBr): Found - %C, 49.27; %H, 3.76; %N, 5.04; %O, 11.92; %Br, 30.01; Calculated for $C_{11}H_{10}NO_2Br$: %C, 49.28; %H, 3.76; %N, 5.22; %O, 11.94; %Br, 29.80.

HRMS (EI): (*m/z*) 267.9651 ($[M]^+$; 60%), 269.4657 ($[M+2]^+$; 60%); Calculated mass for $C_{11}H_{10}NO_2Br$; 268.1066, Observed mass for $C_{11}H_{10}NO_2Br$; 268.7154.

5. Preparation of *N*-phenyl(3-bromo-3-methyl)succinimide (**3a**-Br):

To the solution of **III** or **IV** (2 g, 0.01 mol) in 50 mL of DCM, HBr gas was purged for 24h at room temperature in absence of benzoyl peroxide. The stirring was continued for 12h. The crude product obtained by concentrating the reaction mixture using rotary evaporator purified by column chromatography using petroleum ether and diethyl ether as solvent system followed by

crystallization from DCM and hexane. The compound was dissolved in minimum amount of DCM and hexane was added drop wise till the solution was turbid. The mixture was then kept in ice to get crystals of **3a**-Br (1.3 g, Yield 65%, mp 109 °C).

IR (KBr, cm^{-1}): 3048 (aromatic C-H stretch), 1751 and 1714 (>C=O of imide), 1591, 1501 and 1452 (aromatic >C=C< stretch), 760 (oop C-H bending), 512 (C-Br stretch).

^1H NMR ($CDCl_3$) δ: 7.3 (m, 1 H, C_6H_5), 7.4 (m, 2 H, C_6H_5), 7.5 (m, 2 H, C_6H_5), 3.5 (d, 1 H, ^1J = 18.8 Hz, CH_2), 3.2 (d, 1 H, ^1J = 18.8 Hz, CH_2), 2.1 (s, 3 H, CH_3).

^{13}C NMR (125 MHz, $CDCl_3$) δ: 174.74 and 171.65, 131.47, 129.34, 129.04 and 126.26 (C_6H_5), 51.29 (C-Br), 47.68 (CH_2), 27.47 (CH_3).

Elemental analysis (CHNOBr): Found - %C, 50; %H, 3.82; %N, 5.36; %O, 12.05 %Br, 28.77; Calculated for $C_{11}H_{10}NO_2Br$: %C, 49.28; %H, 3.76; %N, 5.22; %O, 11.94; %Br, 29.80.

HRMS (EI): (*m/z*) 267.8351 ($[M]^+$; 25%), 269.4401 ($[M+2]^+$; 25%); Calculated mass for $C_{11}H_{10}NO_2Br$; 268.1066, Observed mass for $C_{11}H_{10}NO_2Br$; 268.5376.

The FT-IR, ^1H, ^{13}C NMR and HRMS of synthesized compounds **1a**-Br, **2a**-Br, and **3a**-Br are given in the Supporting Information Figure S5 to Figure S16.

C. Synthesis of Copolymers of PI and MMA Using *N*-phenyl(3-bromo-3-methyl)succinimide as Initiator

The reaction scheme for the synthesis of copolymers of PI and MMA using AGET - ATRP is shown in **Scheme 4**. The solution of PI (1.87g, 0.01 mol) and MMA (4.0 mL, 0.04 mol) in 10 mL of dry anisole was taken in three-way 100 mL round bottom flask equipped with reflux condenser and a magnetic bead. To the reaction mixture $CuBr_2$ (56 mg, 0.25 mmol), $Sn(EH)_2$ (41 µL, 0.125 mmol) and 2,2'-bipyridine (117.14 mg, 0.75 mmol) were added. The reaction mixture was freezed under nitrogen, thawed and degassed under vacuum. This cycle was repeated twice. **3a**-Br (67 mg, 0.25 mmol) dissolved in 4 mL of dry anisole, which in a separate two way 100 mL round bottom flask was degassed by subjecting to freeze-pump-thaw cycle twice, was then charged to this reaction flask through a nitrogen purged syringe. The mixture was again subjected to freeze-thaw-vacuum cycle thrice. The reaction flask was now immersed in hot oil bath maintained at 80 °C. The polymerization was terminated by adding the reaction mixture in excess of methanol. The copolymer precipitated out was filtered and washed with hot methanol

to remove any unreacted monomers. The obtained copolymer was dissolved in 100 mL acetone and passed through the alumina bed to remove the catalyst. It was concentrated using rotary evaporator and reprecipitated with methanol. The obtained copolymer was dried under vacuum. The final yield of the copolymers was obtained using gravimetric method. The reactions under similar condition were carried out in ten different reactions flasks and quenched at different time intervals i.e. 5h, 10h, 15h, 20h, 25h, 30h, 35h, 45h, and 50h.

D. Determination of ATRP Equilibrium Constant (K_{ATRP})

The K_{ATRP} of the studied alkyl bromides were determined using Equations 4 and 5. In these equations the parameters I_0 and C_0 are known and Y = [BrCu^{II}Bpy] and k_t are determined as follows.

Determination of [BrCu^{II}Bpy]

To a dry three way round bottom flask dry acetonitrile (30 mL) was added and nitrogen was bubbled for five min. Cu^{I}Br (15.06 mg, 3.7mM) and the ligand Bpy (32.80 mg, 7.0 mM) were then added to the flask and the contents were stirred for 30 minutes to ensure complete dissolution of Cu^{I}Br and formation of complex, the absorbance of the obtained solution (at λ = 745 nm for BrCu^{II}Bpy complex) was set to zero. To this solution **4**-Br (70 mM, 308 µL) was added and the resulting mixture was stirred at room temperature (25 ºC). The absorbance of this solution was measured after every 15 min. A linear increase in the absorbance was observed showing the increase in the concentration of the (BrCu^{II}Bpy complex). The similar experiment was repeated using 50 mM of **4**-Br.

Similarly, the experiments were performed using all other synthesized alkyl bromides viz. **1a**-Br, **2a**-Br and **3a**-Br, at two different concentrations (i.e. 70 mM and 50 mM).The plots of absorbance vs time at 745 nm are given in Supporting Information Figure S17 to Figure S20. The concentration of the BrCu^{II}Bpy complex was determined using values of the extinction coefficient for the complex BrCu^{II}Bpy, which was determined separately.

To determine the extinction coefficient, different solutions of known concentrations, ranging from 0.2 mM to 4.6 mM, of BrCu^{II}Bpy complex in acetonitrile were prepared. The absorbance for each solution was measured using quartz cuvette at λ_{max} = 745 nm. The extinction coefficient calculated from the slope of the curve in the plot of concentration vs absorbance (Supporting Information Figure S21) was found to be 327 $M^{-1}cm^{-1}$.

Determination of Termination Rate Constant (k_t)

In literature[37], a constant value (2.5×10^9 $M^{-1}s^{-1}$) of k_t has been assumed for small radical in the calculation of K_{ATRP}. However a more accurate value can be calculated theoretically using the following formula[38]

$$2k_t^D = 3.78 \times 10^{21} \times D \times d \text{ .....(10)}$$

Where, D is the diffusion coefficient of the radical in a given medium and d is the reaction distance. The later parameter can be approximated, using the approach of Gorrell and Dubois,[19,39] according to the equation,

$$d = \left(\frac{V_m}{N_A}\right)^{1/3} \text{.....(11)}$$

where, V_m is the molar formula of a stable model compound structurally resembling the radical and N_A is Avogadro's number. We used *N*-phenylsuccinimide (SI) as our model compound for the above synthesized alkyl halides. Taking its molecular weight (M = 175.18 g/mol), density (ρ = 1.28 g/cm^3), the molar volume can be calculated as V_m = M/d = 136.97 cm^3/mol, and using equation 11, a value of d = 6.11×10^{-8}cm is obtained. With this estimation of the reaction distance (d), equation 10 can be rewritten (for the phenylsuccinimide radical) as,

$$2k_t^D \approx 2.31 \times 10^{14} \times D \text{.....(12)}$$

The diffusion coefficient, D can be obtained from the classic Einstein - Stokes equation or some of its variations[40] or it can be calculated directly using pulsed field gradient NMR spectroscopic techniques.[41] The latter and more accurate approach was employed in the present study. DOSY allows the measurement of translational diffusion of molecules in solution. The measurement of diffusion is carried out by observing the attenuation of the NMR signals during a pulsed field gradient experiment. The degree of attenuation is a function of the magnetic gradient pulse amplitude and occurs at a rate proportional to the diffusion coefficient of the molecule. In practice, a series of NMR diffusion spectra are acquired as a function of the gradient strength. It can be observed that the intensities of the resonances follow an exponential decay. The slope of this decay is proportional to the diffusion coefficient according to equation,

$$I = I_0 \exp(-D\gamma^2 g^2\delta^2 \Delta - \delta/3 - \pi/2 \text{ .....(13)}$$

where I and I_0 are the signal intensities in the presence and absence of gradient, respectively, γ is the gyromagnetic ratio, g is the strength of the diffusion gradients, D is the diffusion coefficient of the observed spins, δ is the duration of the diffusion gradient and Δ is the diffusion time. All signals corresponding to the same molecular species will decay at the same rate. The processing software evaluates this decay behavior and extracts the diffusion coefficient out of the signal decay curve. In the two dimensional DOSY NMR, spectra are presented with chemical shift along the x-axis and the diffusion constant along the y axis. The DOSY NMR spectrum of SI and its diffusion variable gradient are given in the Supporting Information Figure S22 to Figure S24, respectively. From these data the diffusion coefficient of SI in deuterated acetonitrile was found to be 1.65×10^{-5}cm^2/s. Correspondingly, the value of the termination rate constant $2k_t$ for SI in deuterated acetonitrile at 25 ºC is obtained as 3.81×10^9 $M^{-1}s^{-1}$. This value of $2k_t$ (almost similar constant value used in the literature) is used for the determination of K_{ATRP} values using acetonitrile as solvent for the above synthesized alkyl bromides.

Determination of K_{ATRP} Using UV-Vis-NIR Spectroscopy

The K_{ATRP} values of above synthesized alkyl bromides i.e. **1a**-Br, **2a**-Br, **3a**-Br and commercially available **4**-Br were determined using the modified Fischer - Fukuda equation for the persistent radical effect (equation 4). The values of $F(BrCu^{II}Bpy)$ were obtained by putting the values of concentration of Y, C_0 and I_0 in equation 4. The plots of $F(BrCu^{II}Bpy)$ vs time (t) are linear in nature for all the above mentioned alkyl bromides and these are given in Figure 1 (for 70 mM concentration). Similar plots for concentration of 50 mM are given in Supporting Information Figure S25. The K_{ATRP} values of synthesized alkyl bromides i.e. **1a**-Br, **2a**-Br, **3a**-Br and commercially available **4**-Br were determined from the slope (plot of $F(BrCu^{II}Bpy)$ vs t) and above calculated value of $2k_t$. The results are summarized in Table 1.

RESULTS AND DISCUSSION

In this work we report the synthesis of compounds **1a-**Br and **2a-**Br by the hydrobromination of **III** and **IV**, respectively with HBr gas in presence of benzoyl peroxide at 80 ºC using toluene as solvent, while compound **3a-**Br was synthesized by the hydrobromination of **III** or **IV** with HBr gas in absence of benzoyl peroxide at room temperature using DCM as solvent. The hydrobromination reaction follows Markovnikov's addition (electrophilic addition reaction) of

HBr across the double bond in absence of peroxide and Anti-Markovnikov's addition (free radical addition reaction) of HBr in presence of peroxide.[42]

We also study the bond dissociation enthalpies (BDEs) and other energetic for the four series of alkyl halides **1**, **2**, **3** and **4** (Figure 2) The chosen test set of alkyl halides includes (a) species that mimic the dormant chain ends in the polymerization of PI and MMA (including the synthesized alkyl bromides **1a**-Br, **2a**-Br and **3a**-Br), and (b) some common ATRP initiators (series **4**). The effect of the structure (e.g. primary, secondary and tertiary alkyl halides), substituent and medium on the R–X bond dissociation of these alkyl halides is studied and a comparison of their performance with known potential initiators is evaluated.

All the gas phase optimized geometries (Cartesian coordinates) of the studied compounds and radicals are given in Supporting Information Table S1 and Table S2, respectively.

Structural Features of Alkyl Halides and Alkyl Radicals

We use the B3LYP/ 6-31+G(d)/ LanL2DZ method in our study. This level of theory has been used in the literature for studying similar processes.[20a-20c] To check the accuracy of our computational results, we compare the selected IR frequencies and calculated ^{1}H NMR values with those obtained from experiment for the alkyl bromides **1a-**Br, **2a-**Br and **3a-**Br. Correlation plots between experimentally found and theoretically calculated values of selected IR frequencies and ^{1}H NMR of these alkyl bromides are displayed in Figure 3 and Figure 4 respectively. We found a good correlation between the experimentally found and theoretically calculated IR frequency values (Figure 3, $R^2 = 0.99$) and ^{1}H NMR δ values (Figure 4, $R^2 = 0.99$). This further supports that the chosen method of calculation is quite appropriate for the studied compounds.

The R–X bond distances (r_{R-X}) for the studied compounds in gas phase as well as in two polar solvents are given in Table 2. They are between the ranges 1.809Å to 2.202Å for series **1**, 1.821Å to 2.224Å for series **2**, 1.844Å to 2.261Å for series **3**, and 1.855Å to 2.278Å for series **4** alkyl halides. The R–X bond distances follow the trends **1** < **2** < **3** < **4** for a given X and Cl < Br < I for a given series. The R–X bond lengths systematically increase for all the studied alkyl halides with increasing polarity of the medium and follow the trend gas phase < anisole < acetonitrile for a given R–X. The dihedral angles for the R–X bond with respect to the ring (or with respect to $C(O)OC_2H_5$ for **4**) are between 137°–177° for series **1** and **4**, and between 171°–

172° for series **2** and **3**. The carbon atom bearing the unpaired electron for all the radicals are found to be planar in the sense that the sum of the three bond angles at this carbon are found to be 360° in all cases. The spin densities at this carbon varies from 0.87 to 1.17 in the order **1** > **2** > **3** ≈ **4**.

Homolytic Bond Dissociation Enthalpies and Free Energies

The bond dissociation enthalpy (BDE) data for the studied compounds is displayed in Table 3. They are in the ranges 304.25 kJ/ mol to 170.64 kJ/ mol for series **1**, 263.26 kJ/ mol to 127.72 kJ/ mol for series **2**, 250.70 kJ/ mol to 108.96 kJ/ mol for series **3**, and 257.07 kJ/ mol to 115.16 kJ/ mol for the series **4** alkyl halides in gas phase. The R–X homolytic BDEs of alkyl chlorides are found to be higher than the corresponding alkyl bromides, which are in turn higher than their iodide counterparts. This variation is parallel to the decreasing ionic character of halides, Cl > Br > I. The decrease in BDEs are about 3–22 kJ/ mol from Cl to Br, but about 110–140 kJ/ mol from Br to I, for a given series. For a given halide, the trend in BDEs is **3** ≈ **4** < **2** < **1**, which is nearly according to the stability of the corresponding alkyl free radical generated. The increase is more as we go from series **2** to series **1** than going from **3** to **2** series. For a given series of alkyl halides, the BDEs decrease while the corresponding R–X bond distance increase (Table 2) as we go from X = Cl to X = I. The BDEs correlates well with the R–X bond lengths; as the R–X bond length increase, BDEs decrease (Figure 5). Solvent polarity has different effect for 1° (series **1**) alkyl halides than those of others (2° and 3°) alkyl halides. The trends are gas phase > anisole > acetonitrile for **2**, **3** and **4** series while it is gas phase < anisole < acetonitrile, for series **1** alkyl halides. Thus with increasing polarity of the medium, the relatively-stable radicals (**2**, **3** and **4** series) become more unstable, while the less stable radicals **1** become more stable.

The free energies for the studied alkyl halides (Table 3) are nearly a constant difference with the enthalpy data (about 42 kJ/ mol for series **1**, **2**, **3** and about 48 kJ/ mol for series **4**). This means that the entropy factor contributing for the series **1**, **2** and **3** alkyl halides (and similarly for the series **4)** is nearly same. This is understandable from the structural similarities among alkyl halides of series **1**, **2** and **3**, (and similarly series **4**). The free energies vary according to **4** ≈ **3** < **2** < **1** for a given X and follows the trends Cl > Br > I for a given series. The free energies, like BDEs, increases with decreasing R–X bond lengths. This is obvious from the correlation plot (Figure 6) between the free energies and enthalpies. In presence of polar solvents, the variation of free energies follow the trends, gas phase > anisole > acetonitrile for **2**, **3** and **4** series, while it

is gas phase < anisole < acetonitrile, for series **1** alkyl halides. This trend is similar to the trends found in BDEs.

Relative Equilibrium Constants (K_{ATRP})

As discussed in introduction, the overall equilibrium constant (K_{ATRP}) can be given as product of two equilibrium constants K_{RX} and K_X, the later depends on catalytic system and halogen radical. Thus, for a given catalytic system and a given X, K_X will be a constant, and relative value of K_{ATRP} can be obtained from knowledge of K_{RX}. We have calculated K_{RX} of the alkyl halides from their free energy using standard text book formula.[43] We estimate the $K_X = (K_{ATRP} / K_{RX})$ values for the series **4** alkyl halides from their literature K_{ATRP} values (1.50×10^{-6} for **4**-Cl[7], 3.93×10^{-9} for **4**-Br[15b] and 2.2×10^{-8} for methyl-2-iodopropanoate[7]) and then use this K_X value for the rest of the compounds of a given X. We could have used the K_{ATRP} value of **4**-Br determined experimentally in this work for this purpose. However, for chlorides and iodides we need to use the literature values only. So we decided to use the literature values for all the studied alkyl halides. The values of K_{ATRP}, so obtained, are displayed in Table 4. A quick glance at Table 4 shows that the values of K_{ATRP} for the studied alkyl halides differ in orders of magnitude 10^{-4} to 10^{-16} for gas phase at 25 ºC. All the alkyl halides of series **3** and many from series **2** (**2a-**Cl, **2b**-Cl, **2c**-Cl, **2d**-Cl, **2a-**I, **2b-**I, **2c**-I, **2d**-I) have comparable K_{ATRP} with those of corresponding commercial initiators (series **4**). However, the alkyl halides of series **1** have K_{ATRP} values much smaller than those of series **4** alkyl halides. The K_{ATRP} data follows trends **4** ≈ **3** > **2** >> **1** for a given X and Cl < Br < I for a given series. With increasing temperature from 25 °C to 80 °C, there is order of magnitude increases (10^3 to 10^9) in the values of K_{ATRP}. Different substituent in phenyl ring at para position has no significant effect on bond lengths, bond dissociation enthalpy (BDEs), free energy and K_{ATRP} of **1**, **2**, and **3** series of alkyl halides. The trends of K_{ATRP} in changing medium of the system is gas phase > anisole > acetonitrile for series **1** alkyl halides, and gas phase < anisole < acetonitrile for the rest of alkyl halides (series **2**, **3** and **4**). We obtained good correlation in the variation of K_{ATRP} and R–X bond lengths as well as variation of K_{ATRP} with BDEs. These correlation plots are displayed in Figures 7 and 8, respectively. Figure 7 implies that as the R–X bond length increases -logK_{ATRP} decreases, i.e. logK_{ATRP} increases. This is because as the R–X bond length increases (bond weakens) homolysis is easier and so K_{ATRP} increases. Thus, iodides are better initiators than bromides which in turn are better initiators than

chlorides. However, for a given X the variation of R–X bond length is very little, yet there is an order of magnitude difference in K_{ATRP}. This is mainly due to the structural difference (primary, secondary and tertiary) of alkyl halides. A similar explanation holds for the correlations between BDEs and K_{ATRP} of Figure 8.

The experimentally determined and theoretically calculated values of K_{ATRP} for the studied alkyl bromides are found to be comparable. The reported experimentally calculated K_{ATRP} value for **4**-Br is 3.93×10^{-09}, which is quite comparable with our experimentally calculated value i.e. 1.29×10^{-09}. Similarly, the theoretically calculated K_{ATRP} values in acetonitrile at 25 ºC for **1a**-Br, **2a**-Br and **3a**-Br are 2.77×10^{-18}, 1.37×10^{-11} and 1.42×10^{-09} which are having good agreement with our experimentally determined K_{ATRP} values (1.14×10^{-18}, 1.18×10^{-11} and 1.40×10^{-09}, respectively). The results are summarized in Table 1. All the observations of experimentally determined values of K_{ATRP} for the above mentioned alkyl bromides (using the Fischer - Fukuda equation for the persistent radical effect) are given in Supporting Information Figure S17 to Figure S25.

The K_{ATRP} values of **3a**-Br was found to be comparable with commercially available initiator **4**-Br. Hence, ATRP was carried out using this initiator with the modified procedure (AGET – ATRP) to overcome the sensitivity of the catalyst ($Cu^{I}Br$) towards air and other oxidants.

AGET - ATRP of PI and MMA Using 3a-Br as Initiator

The copolymerization of the monomers PI and MMA was carried out using the mole fraction ratio of 2:8 in presence of $CuBr_2$/ Bpy/ $Sn(EH)_2$ in anisole at 80 ºC using **3a**-Br as initiator. The percent conversion of monomer was calculated gravimetrically by pouring the reaction mixture after 5h, 10h, 15h, 20h, 25h, 30h, 35h, 45h, and 50h in methanol. The copolymer precipitated out was washed with hot methanol, dried and weighed. The FT-IR spectrum of PI - MMA copolymer (Supporting information Figure S26), shows the >C=C< stretching of phenyl ring at 1598, 1501 and 1456 cm^{-1} pinpointing the incorporation of the phenylitaconimide in the copolymer. The absence of characteristic absorption bands at 1663-1665 cm^{-1} due to >C=C< bond stretching shows the absence of monomers. The characteristic absorption bands at 1789 and 1714 cm^{-1} are due to carbonyl groups of imide (>C=O of imide), absorption peak at 1229 cm^{-1} is due to C-O stretching of MMA and 2850 cm^{-1} for C-H stretch of $–CH_3$. In the ^1H NMR spectrum of PI-MMA copolymer in $CDCl_3$ (Supporting Information Figure S27), the peaks in the region δ

= 7.6-7.2 ppm are due to the phenyl ring of PI. The $-OCH_3$ of the side chain is observed at δ = 3.8 ppm, whereas the signal at δ = 3.6 ppm may be attributed to the methylene group adjacent to the carbonyl group of the side chain. Similarly $-CH_3$ of the side chain is observed at δ = 0.8 ppm. The two methylene groups of the polymer backbone are observed in the region δ = 2.8-1.7 ppm and δ = 1.4-0.9 ppm, respectively.

The molecular weights of the copolymers were determined using GPC. The details of the percent conversion of monomers, polydispersity index (PDI) and molecular weights are given in Table 5. A typical linear variation in the plots of % conversion of monomers with time (Figure 9) is observed. This is the characteristic of controlled radical polymerization. Molecular weight of copolymer also increases linearly with % conversion of monomers (Figure 10). The concentration of the unreacted monomer (PI) in the reaction mixture was determined by ^{1}H NMR spectra of the reaction mixture recorded at various time intervals in presence of the known amount of standard 1,1,2,2-tetrachloroethane. For the concentration determination of PI, the intensity of the peaks at δ = 6.5 were compared with the peaks for the standard at δ = 5.9 ppm. A linear plot (Figure 11) is observed for ln $\{[M]_0/[M]_t\}$ vs time, further confirming that the polymerization is occurring under controlled radical polymerization condition. The ^{1}H NMR spectra of the reaction mixture for copolymerization of PI and MMA in $CDCl_3$, at various time intervals are given in Supporting Information Figure S28. The PDI of the copolymer of PI and MMA was found to be 1.30 with 98% of monomer conversion.

Recently, we have reported the ATRP of PI and MMA using **4**-Br as initiator, where we achieve only 50% conversion of monomer with 1.40 PDI for copolymers.[22b] Compared to this, the molecular weight of copolymer, PDI ratio and % conversion of monomer has been improved using **3a**-Br as initiator. In addition, **3a**-Br have better control on polymerization of PI and MMA as compared to **4**-Br.

CONCLUSIONS

We have reported the synthesis of three alkyl bromides (*N*-phenyl(3-bromo-3-methyl)succinimide, *N*-phenyl(3-bromo-4-methyl)succinimide and *N*-phenyl(3-bromomethyl)succinimide) structurally similar to PI for possible chain initiation activity in the ATRP of PI and MMA. The K_{ATRP} of these alkyl bromides along with a commercially available

initiator (ethyl-2-bromoisobutyrate) were determined using UV-Vis-NIR spectroscopy and k_t for radicals using DOSY NMR spectroscopy.

We have also studied the structural and thermodynamic properties (bond dissociation enthalpies and free energies) of these alkyl bromides (along with some similar alkyl halides and some common ATRP initiators) using density functional theory. A variation of substituent in phenyl ring at para position of the studied alkyl halides has very little effect on bond length, bond dissociation enthalpy (BDEs), free energy, and K_{ATRP}. As expected, the R–X bond lengths increase in the order Cl < Br < I for a given R and **4** ≈ **3** < **2** < **1** for a given X, while the BDEs, and free energies follow the opposite trends. With increase in the polarity of the medium, the R–X bond distances increase (BDEs and free energies decrease) for series **2**, **3** and **4**, while opposite trends are observed for series **1** (primary) alkyl halides. Relative values of K_{ATRP} are extracted from the free energy values with respect to common ATRP initiators. It is found that values of K_{ATRP} slightly decrease with increasing solvent polarity and increase significantly with increasing temperature. The value of K_{ATRP} for series **3** and many of the alkyl halides of series **2** (**2a-**Cl, **2b**-Cl, **2c**-Cl, **2d**-Cl, **2a-**I, **2b-**I, **2c**-I, **2d**-I and two of the synthesized bromides **2a**-Br and **3a**-Br) are comparable to commercially available initiator **4**-Br for the ATRP process.

We found a good agreement between our experimentally determined and theoretically calculated K_{ATRP} values of the **4**-Br, **1a**-Br, **2a**-Br, and **3a**-Br in acetonitrile at 25 ºC. The copolymerization of PI and MMA was successfully carried out using one of our synthesized alkyl bromide, **3a**-Br as initiator in anisole at 80 ºC via AGET - ATRP. Comparisons with our recent work on copolymerization of same systems with commercially available initiator **4**-Br, shows that our newly synthesized **3a-**Br has better performance over **4**-Br in terms of control on rate of polymerization, % conversion of monomer and PDI of obtained copolymers.

Supporting Information

Supplementary data associated with this manuscript, FT-IR, ^{1}H, ^{13}C NMR and HRMS spectra of synthesized alkyl bromides, Graphs related to experimental determination equilibrium constant of ATRP and ^{1}H NMR spectra of reaction mixture of copolymers of PI and MMA. B3LYP/ 6-31+G(d)/ LanL2DZ optimized gas phase geometries of all the studied compounds.

Acknowledgements

CD and RC are thankful to DST, New Delhi (Grant No. SR/FT/CS-053/2009) for funding. The support from BITS, Pilani - K. K. Birla Goa Campus is gratefully acknowledged. VSN wishes to thank the UGC, New Delhi for their support under XII Plan grants and Prof. S G Tilve, Department of Chemistry, Goa University for useful discussions.

REFERENCES

1. (a) J. - S. Wang and K. Matyjaszewski, *J. Am. Chem. Soc.*, 1995, **117**, 5614; (b) M. Kato, M. Kamigaito, M. Sawamoto and T. Higashimura, *Macromolecules*, 1995, **28**, 1721; (c) M. Kamigaito, T. Ando and M. Sawamoto, *Chem. Re*v., 2001, **101**, 3689.

2. K. Matyjaszewski and J. Xia, *Chem. Rev.*, 2001, **101**, 2921;

3. (a) K. Matyjaszewski, Ed. Controlled/Living Radical Polymerization, From Synthesis to Materials; ACS Symposium Series 944; American Chemical Society: Washington, DC, 2006; (b) A. D. Jenkins, R. G. Jones and G. Moad, *Pure. Appl. Chem.*, 2010, **82**, 483.

4. (a) K. Matyjaszewski, *Macromolecules*, 2012, **45**, 4015; (b) D. J. Siegwart, J. K. Oh and K. Matyjaszewski, *Prog. Polym. Sci.*, 2012, **37**, 18.

5. (a) K. Matyjaszewski, Ed. Controlled/Living Radical Polymerization, Progress in ATRP, NMP, and RAFT; ACS Symposium Series 768; American Chemical Society: Washington, DC, 2000; (b) C. J. Hawker, A. W. Bosman and E. Harth, *Chem. Rev.*, 2001, **101**, 3661; (c) C. Barner-Kowollik, T. P. Davis, J. P. Heuts, M. H. Stenzel, P. Vana and M. Whittaker, *J. Polym. Sci., Part A: Polym. Chem.*, 2003, **41**, 365.

6. N. V. Tsarevsky and K. Matyjaszewski, *Chem. Rev.*, 2007, **107**, 2270;

7. A. Mullar and K. Matyjaszewski, Radical polymerization, *Controlled and Living Polymerization*, WILEY-VCH Verlag GmbH and Co. KGaA, Weinheim, 2009, pp. 103-166.

8. (a) T. Otsu, *J. Polym. Sci., Part A: Polym. Chem.*, 2000, **38**, 2121; (b) W. Zhang, C. Wang, D. Li, Q. Song, Z. Cheng and X. Zhu, *Macromol. Symp.*, 2008, **261**, 23; (c) R. Nicolay, Y. Kwak and K. Matyjaszewski, *Macromolecules*, 2008, **41**, 4585.

9. W. A. Braunecker and K. Matyjaszewski, *Prog. Polym. Sci.*, 2007, **32**, 93.

10. (a) M. E. Levere, N. H. Nguyen and V. Percec, *Macromolecules*, 2012, **45**, 8267; (b) N. H. Nguyen, M. E. Levere, J. Kulis, M. J. Monteiro and V. Percec, *Macromolecules*, 2012, **45**, 4606; (c) M. Zhong and K. Matyjaszewski, *Macromolecules*, 2011, **44**, 2668; (d) Y. Wang, M. Zhong, Y. Zhang and A. J. D. Magenau, *Macromolecules*, 2012, **45**, 8929; (e) Y. Wang, N. Soerensen, M. Zhong, H. Schroeder, M. Buback and K. Matyjaszewski, *Macromolecules*, 2013, **46**, 683.

11. (a) W. Tang and K. Matyjaszewski, *Macromolecules*, 2007, **40**,1858; (b) B. M. Rosen and V. Percec, *J. Polym. Sci., Part A: Polym. Chem.*, 2008, **46**, 5663.

12. G. Odian, *Principles of Polymerization*, Wiley Interscience, Staten Island, 4th Edition, 2004, pp198-349.

13. G. Moineau, P. Dubois, R. Jerome, T. Senninger and P. Teyssie, *Macromolecules*, 1998, **31**, 545.

14. (a) W. Jakubowski and K. Matyjaszewski, *Macromolecules*, 2005, **38**, 4139; (b) K. Min, H. F. Gao and K. Matyjaszewski, *J. Am. Chem. Soc.*, 2005, **127**, 3825; (c) K. Min, H. F. Gao and K. Matyjaszewski, *J. Am. Chem. Soc.*, 2006, **128**,10521.

15. (a) T. Pintauer, P. Zhou and K. Matyjaszewski, *J. Am. Chem. Soc.*, 2002, **124**, 8196; (b) W. Tang, N. V. Tsarevsky and K. Matyjaszewski, *J. Am. Chem. Soc.*, 2006, **128**, 1598; (c) W. Tang, Y. Kwak, W. Braunecker, N. V. Tsarevsky, M. L. Coote and K. Matyjaszewski, *J. Am. Chem. Soc.*, 2008, **130**, 10702; (d) D. A. Singleton, D. T. Nowlan, N. Jahed and K. Matyjaszewski, *Macromolecules*, 2003, **36**, 8609; (e) I. Degirmenci, S. Eren and V. Aviyente, *Macromolecules*, 2010, **43**, 5602; (f) A. P. Haehnel, M. Schneider-Baumann, K. U. Hiltebrandt, A. M. Misske and C. Barner-Kowollik, *Macromolecules*, 2013, **46**, 15.

16. (a) M. L. Coote, *Macromol. Theory. Simul.*, 2009, **18**, 388; (b) M. D. Miller and A. J. Holder, *J. Phys. Chem. A*, 2010, **114**, 10988.

17. K. Matyjaszewski, T. E. Patten and J. Xia, *J. Am. Chem. Soc.*, 1997, **119**, 674.

18. (a) H. Zang, B. Klumperman, W. Ming, H. Fischer and R. Linde, *Macromolecules*, 2001, **34**, 6169; (b) K. Ohno, Y. Tsujii, T. Miyamoto, T. Fukuda, M. Goto, K. Kobayashi, T. Akaike, *Macromolecules*, 1998, **31**, 1064; (c) H. Fischer, *Chem. Rev.*, 2001, **101**, 3581; (d) A. Goto and T. Fukuda, *Prog. Polym. Sci.*, 2004, **29**, 329; (e) H. Fischer, *J. Polym. Sci., Part A: Polym. Chem.*, 1999, **37**, 1885.

19. (a) W. A. Braunecker, N. V. Tsarevsky, A. Gennaro and K. Matyjaszewski, *Macromolecules*, 2009, **42**, 6348; (b) M. Horn and K. Matyjaszewski, *Macromolecules*, 2013, 46, 3350-3357.

20. (a) M. B. Gillies, K. Matyjaszewski, P-O. Norrby, T. Pintauer, R. Poli and P. Richard, *Macromolecules*, 2003, **36**, 8551; (b) C. Y. Lin, M. L. Coote, A. Gennaro and K. Matyjaszewski, *J. Am. Chem. Soc.*, 2008, **130**, 12762; (c) T. Guliashvili and V. Percec, *J. Polym. Sci., Part A: Polym. Chem.*, 2007, **45**, 1607; (d) C. Y. Lin, S. R. A. Marque, K. Matyjaszewski and M. L. Coote, *Macromolecules*, 2011, **44**, 7568.

21. (a) Z. Hu, X. Shen, H. Qiu, G. Lai, J. Wu and W. Li, *Eur. Polym. J.*, 2009, **45**, 2313; (b) H. Jiang, L. Zhang, J. Pan, X. Jiang, Z. Cheng and X. Zhu, *J. Polym. Sci., Part A: Polym. Chem.*, 2008, **50**, 2244; (c) H. Tang, M. Radosz and Y. Shen, *Macromol. Rapid Commun.*, 2006, **27**,

1127; (d) J. Mosnacek and M. Ilcikova, *Macromolecules*, 2012, **45**, 5859; (e) N. Chan, M. F. Cunningham and R. A. Hutchinson, *Macromol. Chem. Phys.*, 2008, **209**, 1797.

22. (a) C. Deoghare, R. N. Behera and R. Chauhan, **"**Controlled Radical Polymerization of *N*-phenylitaconimide with Methyl Methacrylate: Experimental and Theoretical Study" presented in 3rd FAPS Polymer Congress MACRO 2013, May 15-18, 2013, Bangalore, India; (b) C. Deoghare, P. C. Deb, C. Baby, R. N. Behera and R. Chauhan, "Controlled Radical Copolymerization of *N*-phenylitaconimide with Methyl Methacrylate via Atom Transfer Radical Polymerization" (Communicated to *J. Appl. Polym. Sci.*, manuscript reference number APP-2014-05-1917).

23. V. Anand and V. Choudhary, *J. Appl. Polym. Sci*., 2003, **89**, 1195.

24. (a) V. Anand and V. Choudhary, *J. Appl. Polym. Sci.*, 2001, **82**, 2078; (b) R. Chauhan and V. Choudhary, *J. Appl. Polym. Sci.*, 2010, **115**, 491.

25. (a) P. Bonnarme, B. Gillet, A. M. Sepulchre, C. Role, J. C. Beloeil and C. Ducrocq, *J. Bacteriol.*, 1995, **177**, 3573; (b) K. Yahiro, S. Shibata, S-r. Jia, Y. Park and M. Okabe, *J. Ferment. Bioeng.*, 1997, **84**, 375; (c) C. S. K. Reddy and R. P. Singh, *Bioresource Technol.*, 2002, **85**, 69.

26. (a) K. N. Ninan, R. George, K. Krishnan and K. V. C. Rao, *J. Appl. Polym. Sci.*, 1989, **37**, 127; (b) Qiu, K. Y and Zhao T. *Polym. Inter.*, 1995, **38**, 71; (c) A. Solanki, V. Choudhary and I. K. Varma, *J. Appl. Polym. Sci.*, 2002, **84**, 2277.

27. (a) C. C. Price and E. C. Coyner, *J. Am. Chem. Soc.*, 1940, **62**, 1306; (b) O. Cakmak, I. Kahveci, I. Demirtas, T. Hökelek, and K. Smith, *Collect. Czech. Chem. Commun.*, 2000, **65**, 1791.

28. E. O. Stejskal, and J. E. Tanner, *J. Chem. Phys*., 1965, **42**, 288.

29. D. Wu, A. Chen, and C.S. Johnson Jr., *J. Magn. Reson. A*, 1995, **123**, 115.

30. C.S. Johnson Jr., *Prog. NMR Spectr.*, 1999, **34**, 203.

31. Gaussian 09, Revision B.01, M. J. Frisch, G. W. Trucks, H. B. Schlegel, G. E. Scuseria, M. A. Robb, J. R. Cheeseman, G. Scalmani, V. Barone, B. Mennucci, G. A. Petersson, H. Nakatsuji, M. Caricato, X. Li, H. P. Hratchian, A. F. Izmaylov, J. Bloino, G. Zheng, J. L. Sonnenberg, M. Hada, M. Ehara, K. Toyota, R. Fukuda, J. Hasegawa, M. Ishida, T. Nakajima, Y. Honda, O. Kitao, H. Nakai, T. Vreven, J. A. Montgomery, Jr., J. E. Peralta, F. Ogliaro, M. Bearpark, J. J. Heyd, E. Brothers, K. N. Kudin, V. N. Staroverov, T. Keith, R. Kobayashi, J.

Normand, K. Raghavachari, A. Rendell, J. C. Burant, S. S. Iyengar, J. Tomasi, M. Cossi, N. Rega, J. M. Millam, M. Klene, J. E. Knox, J. B. Cross, V. Bakken, C. Adamo, J. Jaramillo, R. Gomperts, R. E. Stratmann, O. Yazyev, A. J. Austin, R. Cammi, C. Pomelli, J. W. Ochterski, R. L. Martin, K. Morokuma, V. G. Zakrzewski, G. A. Voth, P. Salvador, J. J. Dannenberg, S. Dapprich, A. D. Daniels, O. Farkas, J. B. Foresman, J. V. Ortiz, J. Cioslowski and D. J. Fox, Gaussian, Inc., Wallingford CT, 2010.

32. C. Lee, W. Yang and R. G. Parr, *Phys. Rev.*, 1988, **B37**, 785; (b) A. D. Becke, *Phys. Rev.*, 1988, **A38**, 3098; (c) A. D. Becke, *J. Chem. Phys.*, 1993, **98**, 5648.

33. J. B. Foresman and A. Frisch, *Exploring chemistry with electronics structure methods*, Gaussian, Inc. Pittsburgh, 2nd edition,1996, pp. 64.

34. C. E. Moore, Atomic Energy Levels, US Government Printing Office, Washington, DC, 1952, Vols. I–III.

35. S. Miertus, E. Scrocco and J. Tomasi, *Chem. Phys.*, 1981, **55** 117.

36. V. Anand, S. Agarwal, A. Greiner and V. Choudhary, *Polym. Int.*, 2005, **54**, 823.

37. (a) H. Fischer and P. Henning, *Acc. Chem. Res.*, 1987, **20**, 200; (b) H. Fischer and L. Radom, *Angew. Chem. Int. Ed.*, 2001, **40**, 1340.

38. H. H. Schuh and H. Fischer, *Hel. Chim. Acta.*, 1978, **61**, 2130.

39. J. H. Gorrell and J. T. Dubois, *Trans. Faraday Soc.*, 1967, **63**, 347.

40. (a) H. A. Kooijman, *Ind. Eng. Chem. Res.*, 2002, **41**, 3326; (b) In-C. Yeh and G. Hummer, *J. Phys. Chem. B*, 2004, **108**, 15873.

41. (a) T. Brand, E. J. Cabrita and S. Berger, *Prog. NMR Spectr.*, 2005, **46**, 159; (b) Y. Cohen, L. Avram and L. Frish, *Angew. Chem. Int. Ed.*, 2005, **44**, 520; (c) P. S. Pregosin, P. G. Anil Kumar and I. Fernandez, *Chem. Rev.*, 2005, **105**, 2977.

42. (a) M. S. Kharasch and W. M. M. Potts, *J. Org. Chem.*, 1937, **02**, 195; (b) M. S. Kharasch, H. Engelmann and F. R. Mayo, *J. Org. Chem.*, 1937, **02**, 288; (c) M. S. Kharasch and M. C. McNab, *J. Am. Chem. Soc.*, 1934, **56**, 1425; (d) M. S. Kharasch, A. John and Jr. Hinckley, *J. Am. Chem. Soc.*, 1934, **56**, 1243.

43. P. Atkins and J. de Paula, *Physical Chemistry*, W. H. Freeman and Company, United States, 9th Edition, 2010, pp. 217.

Figure 1. Plots of $F(Y) = F[BrCu^{II}Bpy]$ vs time (s) for the alkyl bromides at 70 mM, (a) **4**-Br, (b) **1a**-Br, (c) **2a**-Br and (d) **3a**-Br.

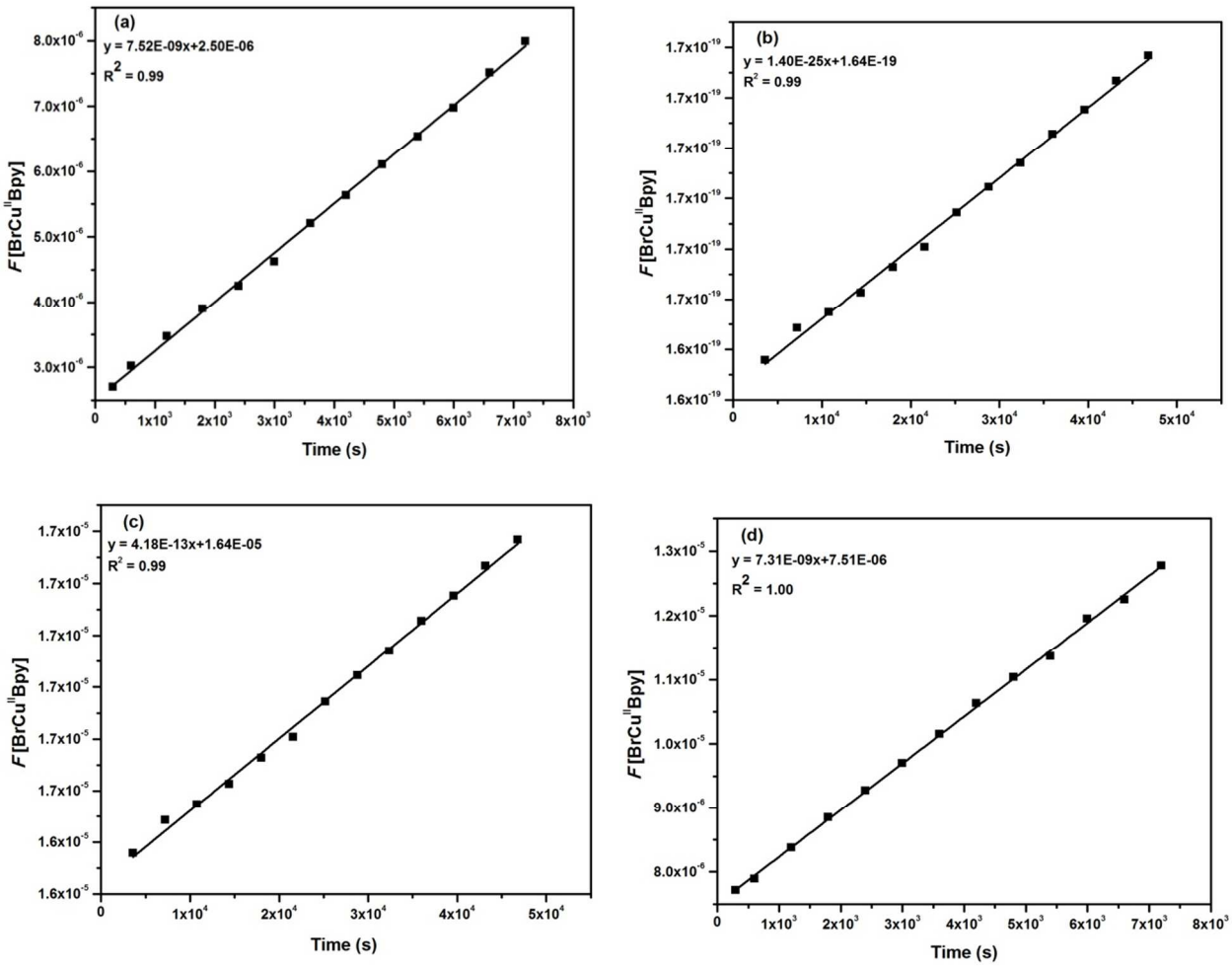

Figure 2.The alkyl halides, **1** (**1a-**X to **1d-**X), **2** (**2a-**X to **2d-**X), **3** (**3a-**X to **3d-**X) and **4-**X (X = Cl, Br, I) investigated in this study.

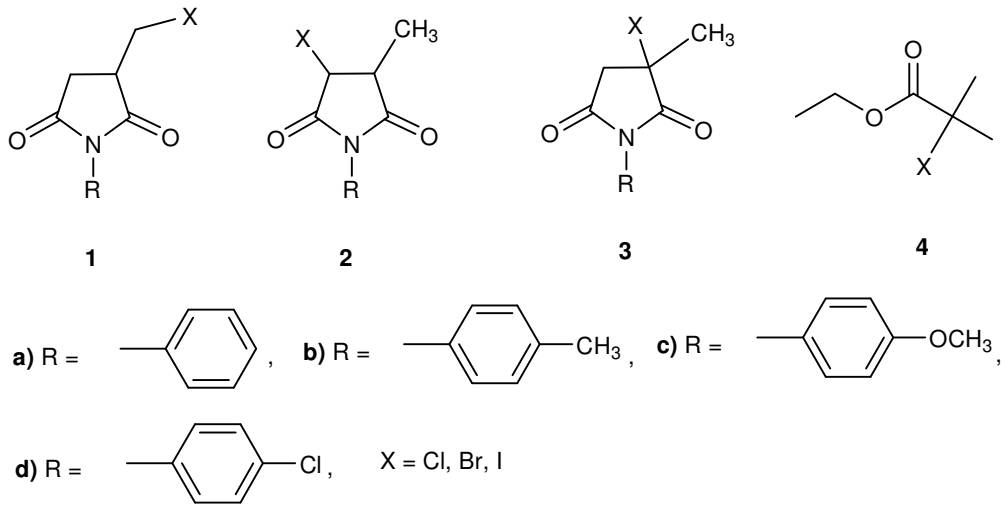

Figure 3. Correlation plot of theoretical and experimental values of selected IR frequencies (in cm^{-1}) of the studied alkyl bromides. Frequencies corresponding to C-C (both aliphatic and aromatic), C=C (aromatic), C-H (both aliphatic and aromatic), C=O, C-N and C-Br are considered.

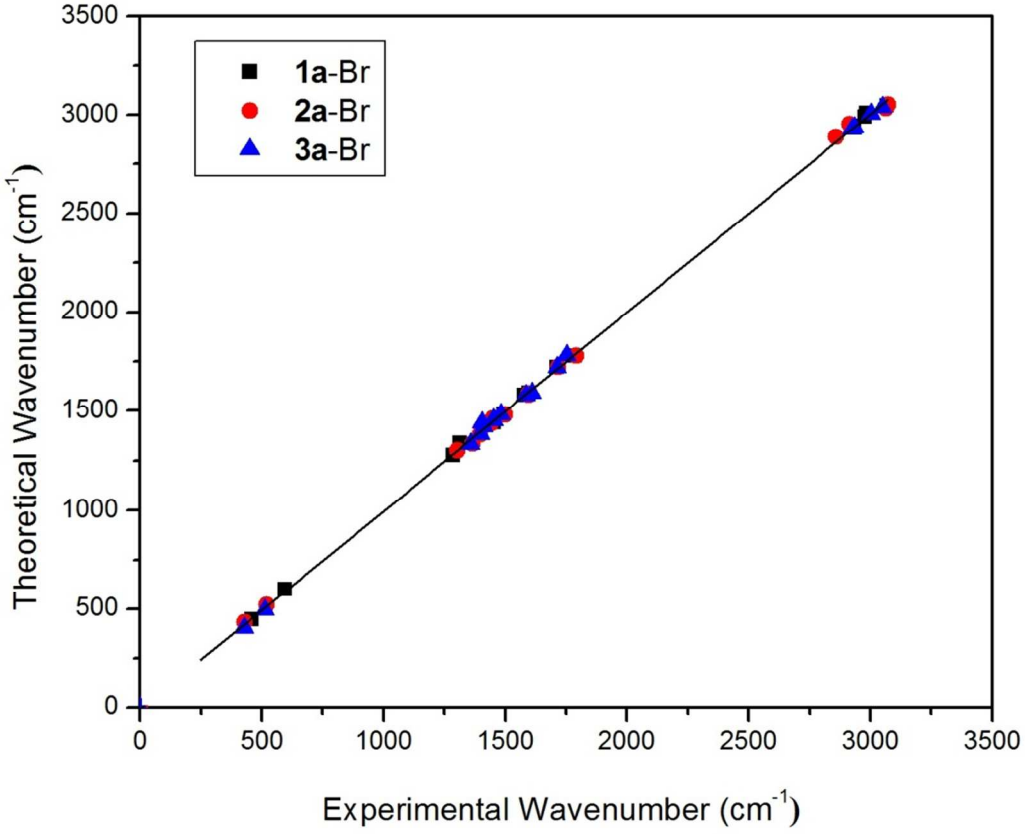

Figure 4. Correlation plot of theoretical and experimental δ (in ppm) values of ^{1}H NMR of studied alkyl bromides.

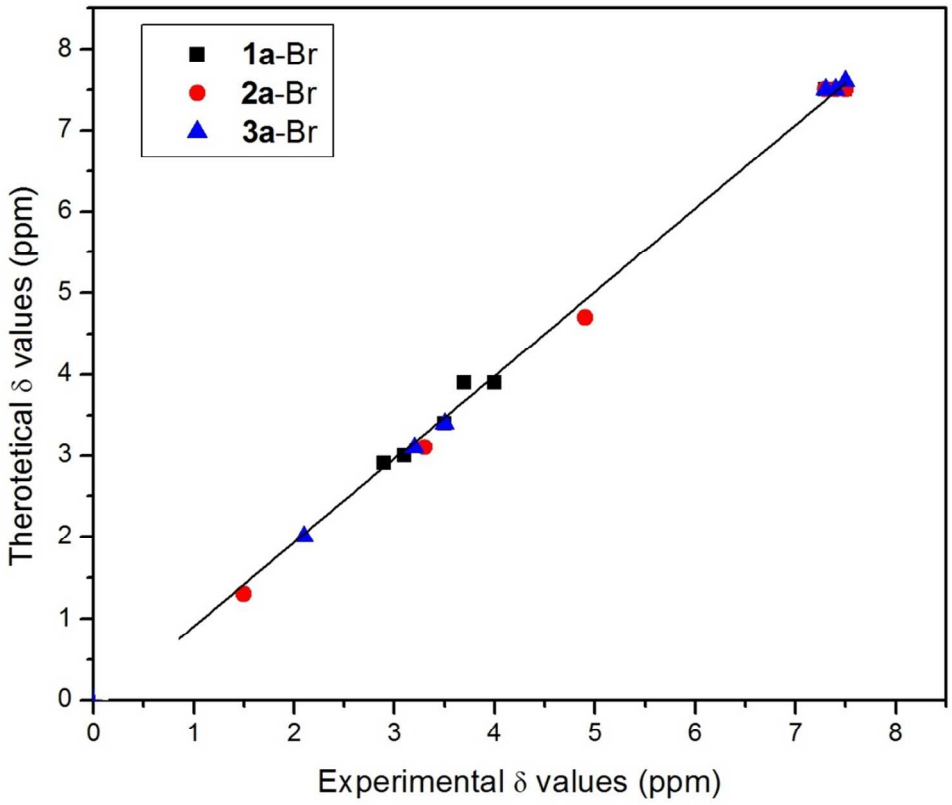

Figure 5. Correlation plot of bond dissociation enthalpies with R–X bond distances of the studied alkyl halides.

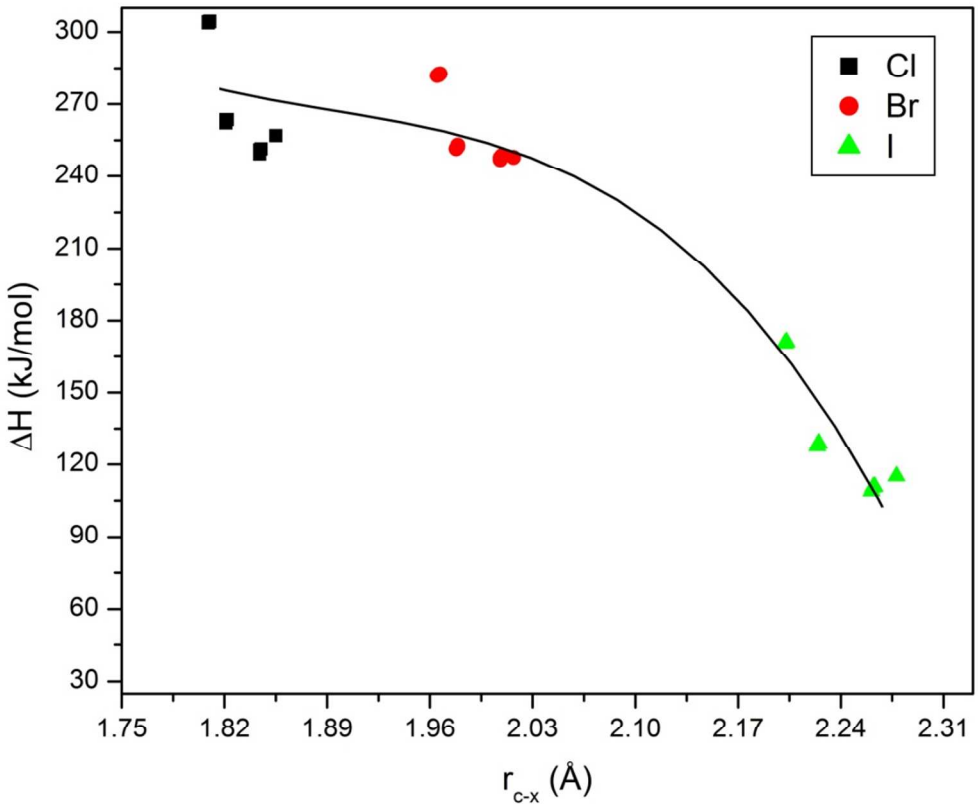

Figure 6. Variation of enthalpies with the free energies for the R–X bond dissociation process for the studied alkyl halides.

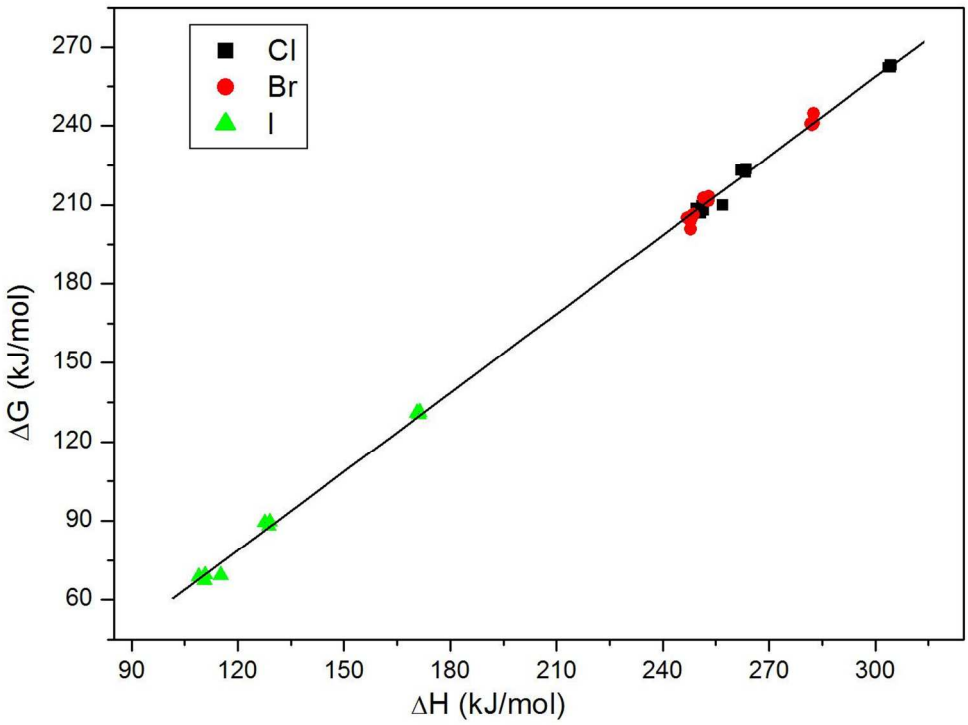

Figure 7. Correlation plot of relative K_{ATRP} values with R–X bond lengths for the studied alkyl halides.

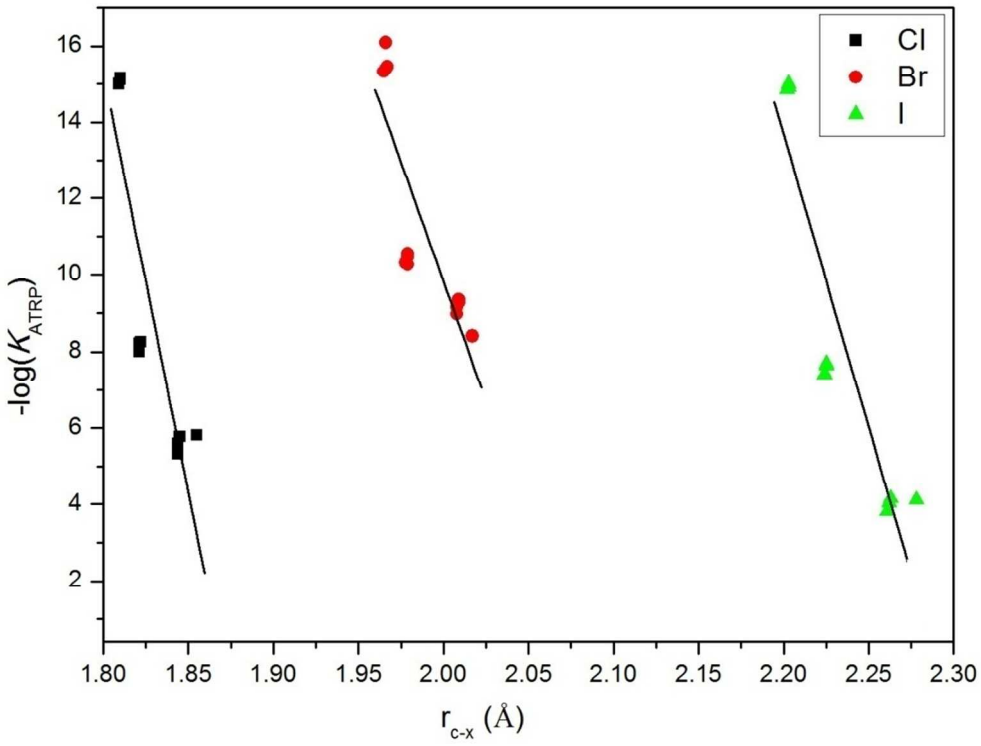

Figure 8. Correlation plot of relative K_{ATRP} values with R–X bond enthalpies of studied alkyl halides.

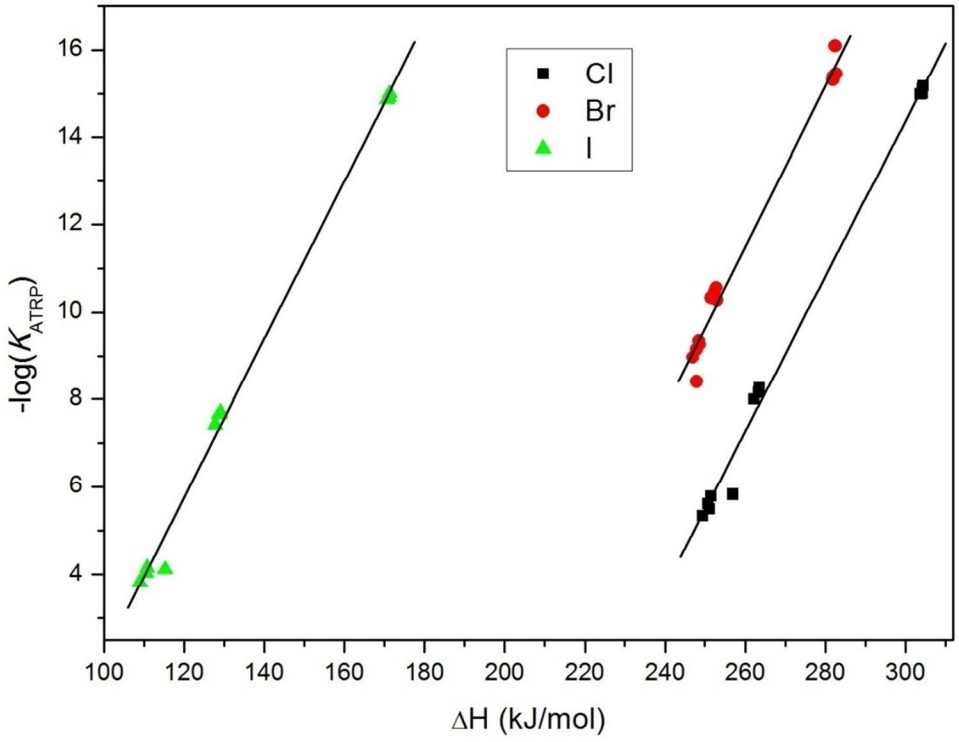

Figure 9. Plot of % conversion of monomer with time for AGET - ATRP of PI and MMA. Experimental conditions: [PI]/[MMA]/[**3a**-Br]/[$CuBr_2$]/[Bpy]/[$Sn(EH)_2$] = 20/80/1/1/3/0.5, in anisole at 80 ºC.

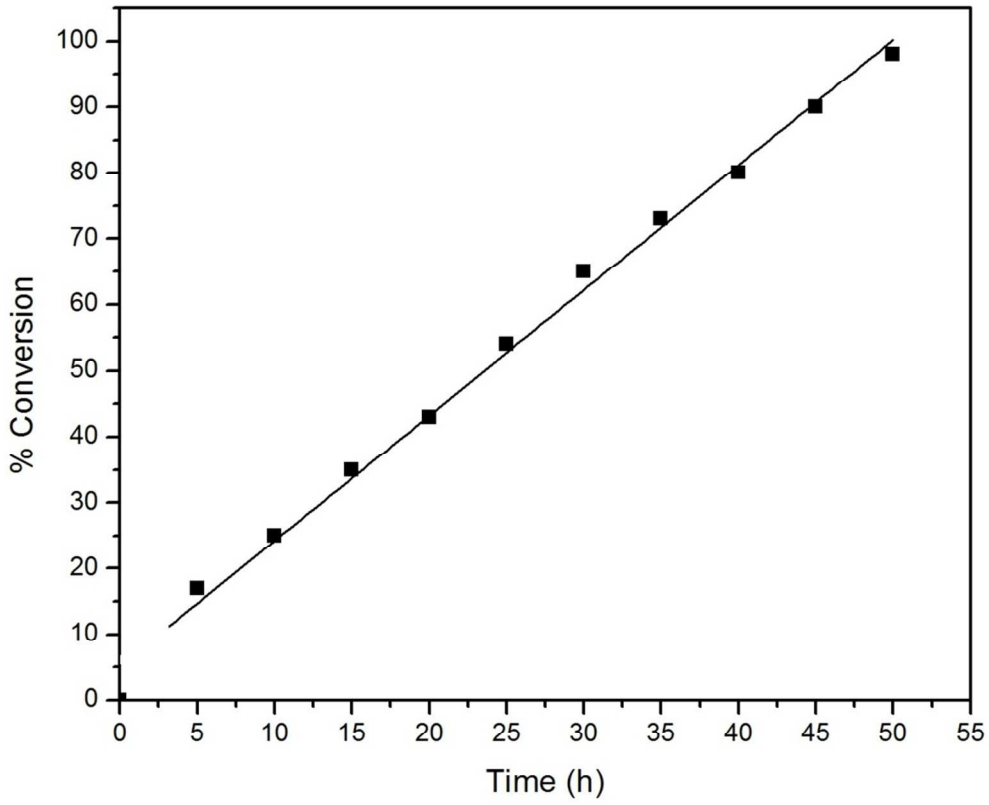

Figure 10. Plot of molecular weight of copolymer with % conversion of monomer for AGET - ATRP of PI and MMA. Experimental conditions: [PI]/[MMA]/[**3a**-Br]/[$CuBr_2$]/[Bpy]/[$Sn(EH)_2$] = 20/80/1/1/3/0.5, in anisole at 80 ºC.

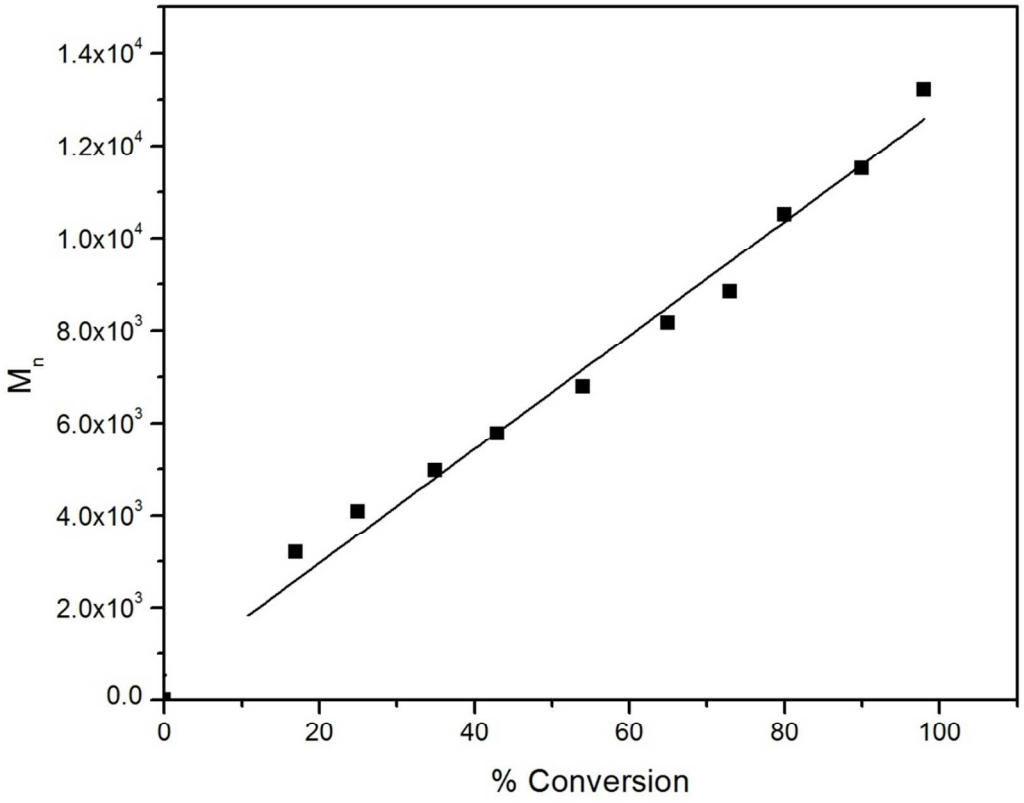

Figure 11. Plot of ln {$[M]_0/[M]_t$} with time for AGET - ATRP of PI and MMA. Experimental conditions: [PI]/[MMA]/[**3a**-Br]/[$CuBr_2$]/[Bpy]/[$Sn(EH)_2$] = 20/80/1/1/3/0.5, in anisole at 80 ºC.

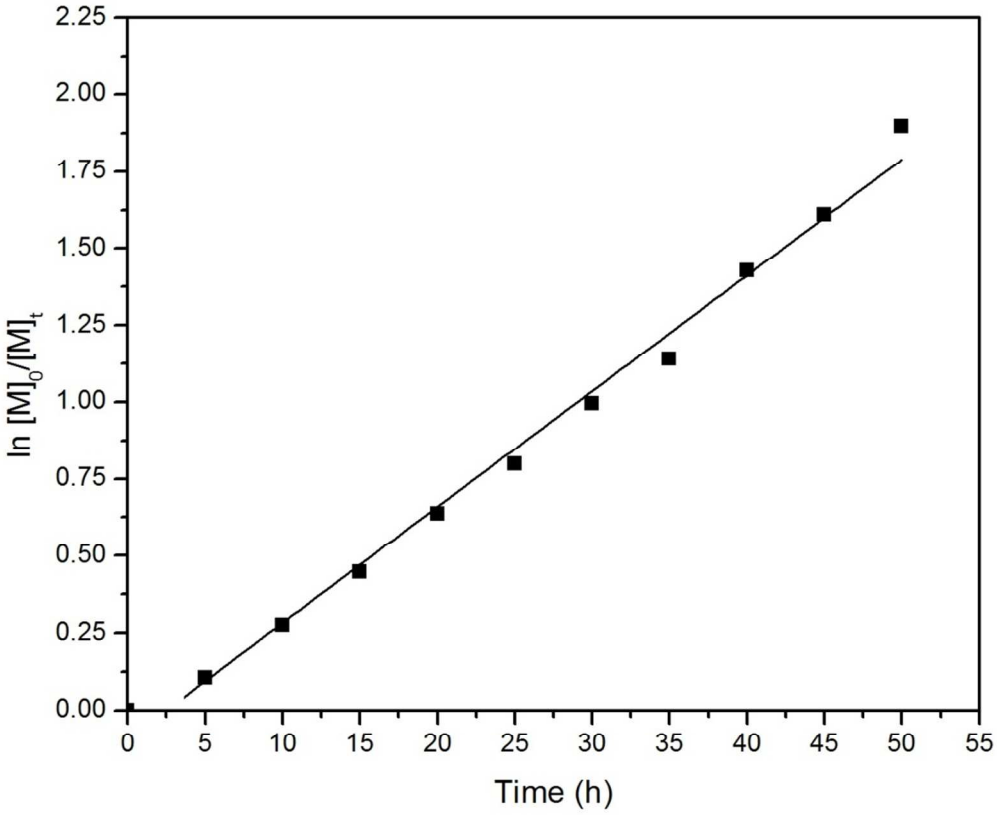

Table 1. The K_{ATRP} values for R–X homolytic bond cleavage of studied alkyl bromides in acetonitrile at 25 ºC using UV-Vis-NIR spectroscopy. Experimental conditions: [R–X]:[CuBr]:[Bpy] = 70 and 50 mM: 3.5 mM: 7.0 mM. The K_{ATRP} values, calculated using DFT method, are given in last column.

R-X	K_{ATRP} at 70 mM	K_{ATRP} at 50 mM	Average K_{ATRP}	K_{ATRP} Calculated
4-Br	1.40×10^{-09}	1.18×10^{-09}	1.29×10^{-09}	3.93×10^{-09}
1a-Br	0.89×10^{-18}	1.39×10^{-18}	1.14×10^{-18}	2.77×10^{-18}
2a-Br	1.07×10^{-11}	1.29×10^{-11}	1.18×10^{-11}	1.37×10^{-11}
3a-Br	1.39×10^{-09}	1.40×10^{-09}	1.40×10^{-09}	1.42×10^{-09}

Table 2. The R–X bond lengths of studied alkyl halides in gas phase and in the solution phase at 25 °C.

R-X	r_{R-X} (Å)		
	Gas	Anisole	Acetonitrile
1a-Cl	1.809	1.817	1.822
1a-Br	1.966	1.973	1.977
1a-I	2.203	2.210	2.213
1b-Cl	1.810	1.818	1.822
1b-Br	1.966	1.973	1.977
1c-Cl	1.810	1.818	1.822
1c-Br	1.967	1.974	1.977
1c-I	2.203	2.267	2.270
1d-Cl	1.809	1.817	1.821
1d-Br	1.965	1.972	1.977
1d-I	2.202	2.202	2.213
2a-Cl	1.821	1.824	1.825
2a-Br	1.979	1.981	1.982
2a-I	2.225	2.227	2.228
2b-Cl	1.821	1.824	1.825
2b-Br	1.979	2.014	2.016
2c-Cl	1.822	1.825	1.826
2c-Br	1.979	1.982	1.982
2c-I	2.225	2.227	2.229
2d-Cl	1.821	1.824	1.825
2d-Br	1.978	1.980	1.981
2d-I	2.224	2.226	2.228
3a-Cl	1.844	1.848	1.850
3a-Br	2.008	2.014	2.016
3a-I	2.262	2.266	2.267
3b-Cl	1.844	1.848	1.849
3b-Br	2.009	2.014	2.016
3c-Cl	1.845	1.849	1.851
3c-Br	2.009	2.013	2.016
3c-I	2.263	2.267	2.270
3d-Cl	1.844	1.847	1.849
3d-Br	2.008	2.013	2.015
3d-I	2.261	2.266	2.269
4-Cl	1.855	1.865	1.869
4-Br	2.017	2.025	2.029
4-I	2.278	2.287	2.292

Table 3. Enthalpy and Free energy for R–X homolytic cleavage of studied alkyl halides in gas phase, and solution phase at 25 °C.

R-X	ΔH (kJ/mol)			ΔG (kJ/mol)		
	Gas	Anisole	Acetonitrile	Gas	Anisole	Acetonitrile
1a-Cl	304.25	309.03	312.42	262.30	267.55	270.73
1a-Br	282.14	285.92	289.09	240.78	243.14	247.92
1a-I	171.1	173.88	176.37	130.99	132.72	135.14
1b-Cl	304.29	306.67	312.67	262.92	273.03	271.26
1b-Br	282.54	284.00	289.42	244.74	254.1	248.66
1c-Cl	304.51	309.27	312.75	263.29	266.56	266.54
1c-Br	282.65	286.18	289.48	241.11	242.47	243.93
1c-I	171.31	174.16	176.77	131.45	133.45	133.62
1d-Cl	303.79	323.71	312.62	262.23	278.44	272.18
1d-Br	281.88	285.78	289.21	240.34	243.22	246.32
1d-I	170.64	173.72	176.46	130.64	134.26	135.03
2a-Cl	263.26	261.18	260.68	223.23	221.16	220.06
2a-Br	252.48	249.94	249.11	212.67	210.36	209.71
2a-I	128.76	126.04	125.23	89.49	87.24	86.62
2b-Cl	263.55	-	260.93	223.58	-	216.27
2b-Br	253.05	-	251.99	211.54	-	200.68
2c-Cl	263.56	261.67	261.14	223.80	222.49	219.97
2c-Br	252.86	250.51	249.56	213.15	212.15	209.36
2c-I	129.05	126.47	125.8	89.70	87.43	87.31
2d-Cl	262.22	260.06	259.76	222.29	220.69	223.86
2d-Br	251.6	248.79	248.34	211.83	208.9	208.93
2d-I	127.72	125.24	124.59	88.14	86.13	85.24
3a-Cl	250.7	247.39	245.92	208.66	204.27	202.69
3a-Br	247.88	243.71	242.06	205.12	199.94	198.21
3a-I	110.61	106.07	104.31	68.86	64.63	64.28
3b-Cl	251.07	247.62	246.46	208.01	204.38	203.1
3b-Br	248.42	244.18	242.59	206.26	199.3	197.32
3c-Cl	251.48	248.16	246.66	209.61	207.29	203.48
3c-Br	248.7	245.02	243.04	205.76	201.86	196.88
3c-I	110.83	106.47	104.8	69.54	64.95	63.82
3d-Cl	249.42	245.81	244.9	207.07	202.72	203.66
3d-Br	246.95	242.58	241.26	204.06	198.95	197.71
3d-I	108.96	104.45	102.84	67.58	62.81	62.26
4-Cl	257.07	255.98	255.53	209.9	208.81	205.31
4-Br	247.87	246.44	245.9	200.87	199.29	195.68
4-I	115.16	112.71	111.66	69.3	66.64	62.98

Table 4. Relative values of K_{ATRP} for R–X homolytic bond cleavage of studied alkyl halides in gas phase and in solution phase.

R-X	K_{ATRP}			
	Gas, 25 °C	Gas, 80 °C	Anisole, 25 °C	Acetonitrile, 25 °C
1a-Cl	9.92×10^{-16}	2.03×10^{-07}	7.68×10^{-17}	5.19×10^{-18}
1a-Br	4.00×10^{-16}	1.86×10^{-08}	8.18×10^{-17}	2.77×10^{-18}
1a-I	1.18×10^{-15}	5.59×10^{-11}	5.30×10^{-11}	6.96×10^{-17}
1b-Cl	7.72×10^{-16}	1.58×10^{-07}	8.40×10^{-18}	4.18×10^{-18}
1b-Br	8.11×10^{-17}	4.32×10^{-09}	9.82×10^{-19}	2.06×10^{-18}
1c-Cl	6.65×10^{-16}	1.38×10^{-07}	1.14×10^{-16}	2.81×10^{-17}
1c-Br	3.50×10^{-16}	1.86×10^{-08}	1.07×10^{-16}	1.39×10^{-17}
1c-I	9.82×10^{-16}	4.71×10^{-11}	1.76×10^{-16}	1.28×10^{-16}
1d-Cl	1.02×10^{-15}	2.03×10^{-07}	9.50×10^{-19}	2.89×10^{-18}
1d-Br	4.78×10^{-16}	2.42×10^{-08}	7.92×10^{-17}	5.30×10^{-18}
1d-I	1.36×10^{-15}	6.25×10^{-11}	1.27×10^{-16}	7.26×10^{-17}
2a-Cl	6.94×10^{-09}	1.07×10^{-01}	1.03×10^{-08}	3.90×10^{-09}
2a-Br	3.36×10^{-11}	2.62×10^{-04}	4.53×10^{-11}	1.37×10^{-11}
2a-I	2.20×10^{-08}	7.21×10^{-05}	2.20×10^{-08}	2.20×10^{-08}
2b-Cl	6.02×10^{-09}	9.45×10^{-02}	-	1.80×10^{-08}
2b-Br	5.31×10^{-11}	2.01×10^{-04}	-	5.25×10^{-10}
2c-Cl	5.50×10^{-09}	8.65×10^{-02}	6.01×10^{-09}	4.04×10^{-09}
2c-Br	2.77×10^{-11}	2.22×10^{-04}	2.20×10^{-11}	1.58×10^{-11}
2c-I	2.02×10^{-08}	6.73×10^{-05}	2.04×10^{-08}	1.67×10^{-08}
2d-Cl	1.01×10^{-08}	1.46×10^{-01}	1.24×10^{-08}	8.42×10^{-10}
2d-Br	4.72×10^{-11}	3.49×10^{-04}	8.16×10^{-11}	1.88×10^{-11}
2d-I	3.79×10^{-08}	1.16×10^{-04}	3.44×10^{-08}	3.84×10^{-08}
3a-Cl	2.47×10^{-06}	$1.72\times10^{+01}$	9.36×10^{-06}	4.30×10^{-06}
3a-Br	7.06×10^{-10}	4.11×10^{-03}	3.03×10^{-09}	1.42×10^{-09}
3a-I	9.05×10^{-05}	9.46×10^{-02}	2.01×10^{-04}	2.00×10^{-04}
3b-Cl	3.22×10^{-06}	$2.30\times10^{+01}$	8.96×10^{-06}	3.65×10^{-06}
3b-Br	4.46×10^{-10}	2.64×10^{-02}	3.93×10^{-09}	2.03×10^{-09}
3c-Cl	1.68×10^{-06}	$1.23\times10^{+01}$	2.77×10^{-06}	3.13×10^{-06}
3c-Br	5.46×10^{-10}	3.35×10^{-03}	1.40×10^{-09}	2.42×10^{-09}
3c-I	6.89×10^{-05}	7.30×10^{-02}	1.76×10^{-04}	2.17×10^{-04}
3d-Cl	4.70×10^{-06}	$3.01\times10^{+01}$	1.75×10^{-05}	2.91×10^{-06}
3d-Br	1.08×10^{-09}	6.17×10^{-03}	4.52×10^{-09}	1.73×10^{-09}
3d-I	1.52×10^{-04}	1.43×10^{-01}	4.19×10^{-04}	4.07×10^{-04}
4-Cl	1.50×10^{-06}	$1.56\times10^{+01}$	1.50×10^{-06}	1.50×10^{-06}
4-Br	3.93×10^{-09}	2.29×10^{-02}	3.93×10^{-09}	3.93×10^{-09}
4-I	7.59×10^{-05}	1.05×10^{-01}	8.93×10^{-05}	3.05×10^{-04}

Table 5. The variation in molecular weight, PDI of copolymer and % conversion of monomer with time for copolymerization of PI and MMA via AGET - ATRP. Experimental conditions: [PI]/[MMA]/[**3a**-Br]/[$CuBr_2$]/[Bpy]/[$Sn(EH)_2$] = 20/80/1/1/3/0.5, in anisole at 80 ºC.

S. No.	Time (h)	Yield (%)	% Conversion	Molecular Weight (M_n) g/mol	PDI
1	5	17.89	17	3292	1.32
2	10	25.89	25	4316	1.56
3	15	34.75	35	4858	1.50
4	20	43.61	43	5086	1.37
5	25	55.03	54	6772	1.32
6	30	64.91	65	7167	1.34
7	35	73.25	73	8174	1.41
8	40	80.40	80	10518	1.53
9	45	90.97	90	12347	1.47
10	50	98.81	98	13224	1.30

Synthesis, Characterization and Computational Study of Potential Itaconimide-based Initiators for Atom Transfer Radical Polymerization

Chetana Deoghare[1], C. Baby[2], Vishnu S. Nadkarni[3], Raghu Nath Behera[1,*] and Rashmi Chauhan[1,*]

Graphical Abstract: We report the synthesis of three possible potential initiators **1a**-Br, **2a**-Br, **3a**-Br for the ATRP of *N*-phenylitaconimide and methyl methacrylate. We found a good agreement between our experimentally determined and theoretically calculated K_{ATRP} values for these initiators. ATRP experiments indicate that **3a-**Br performs better than the commercially available initiator ethyl-α-bromoisobutyrate for our system.